THE ROYAL SOCIETY

A fast algorithm for the simulation of polycrystalline misfits: martensitic transformations in two space dimensions

By Oscar P. Bruno and Guillermo H. Goldsztein

Department of Applied Mathematics, Caltech, Pasadena, CA 91125, USA

Received 4 December 1998; accepted 7 April 1999

We present a fast method for the solution of problems of elasticity involving microscopic misfit strains. While the main case we consider is that associated with martensitic transformations in polycrystals, our methods can be applied to a variety of systems whose constituents undergo misfit deformations, including polycrystalline magnetostriction, thermal expansion, etc., as well as mathematically analogous phenomena in ferroelectricity and ferromagnetism. The basic component of our method is an explicit solution for Eshelby-type problems on square elements. Fast computation of the polycrystal energy results through a rapidly convergent sequence of approximations which can, in fact, be interpreted as a generalization of a class of upper bounds introduced recently. The overall complexity of the method is $\mathcal{O}(N)$ operations, where N is the number of component crystallites. We also present a new lower bound for the energy, giving additional insights on the microscopic phenomena leading to the observed structural behaviour. The present work applies to two-dimensional polycrystals; extensions to the three-dimensional case have been implemented and will be presented elsewhere.

Keywords: polycrystals; nonlinear homogenization; martensitic transformations; elasticity; numerical methods

1. Introduction

We present a fast numerical method for the solution of nonlinear elasticity problems in polycrystals supporting microscopic misfit strains. As examples of polycrystalline misfits we mention: (1) the deformations that take place in polycrystals as a result of solid-to-solid phase transitions and thermal expansion; (2) the electrical or magnetic misfits associated with electro- and magnetorheological materials; and (3) the combined elastic and magnetic–electric misfits which occur in connection with the phenomenon of magnetostriction and electrostriction in composite materials. The methods we introduce here, which we specialize to the case of the martensitic transformation in polycrystals, can be generalized and applied to a variety of problems involving these phenomena. Our algorithms result from consideration of a class of approximations for the elastic energy, which can be evaluated with a reduced operation count, and which converge very fast to the actual minimum energy values. In addition to these approximations and associated numerical algorithms we derive a

class of new *lower bounds*—which give additional insights on the microscopic phenomena leading to the observed structural behaviour.

We thus consider polycrystals whose component crystallites can undergo solid-to-solid martensitic phase transitions as a result of applied stresses or temperature changes. These transitions lead to deformations and associated *transformation strains*. Typically, a single crystal of a given martensitic material will undergo transitions with basic deformations which can be classified into a finite number of *variants* (see Wechsler *et al*. 1953; Wayman 1964; Khachaturyan 1967; Roitburd 1973; Bowles & Mackenzie 1954). These strains can be very large (of the order of 10% in some cases) and they occur as a result of a fundamental change in the crystallographic structure of the alloy. Transformation strains are therefore not elastic strains; rather they are associated with genuine changes in the crystalline structure of the material as it transitions into the transformed state.

The possible transformation strains of a single crystal depend on the orientation of the underlying crystalline lattice. More precisely, a single crystal whose orientation is given by a certain rotation R of the reference crystal will exhibit transformation strains equal to rotated versions, by the same rotation R, of those corresponding to the reference configuration. Thus, as neighbouring not-equally-oriented grains in a polycrystal transform, their shape change will most likely lead to shape mismatches or *misfits*. These misfits can only be accommodated through elastic deformations—thus leading to storage of elastic energy.

Martensitic transformations generally involve both dissipative and conservative processes. Thus, conclusions obtained from considerations based on minimization of the stored elastic energy only apply in regimes in which dissipative effects may either be neglected or accounted for appropriately within the conservative framework. Realistic configurations can often be treated by such methods (Leo *et al*. 1995; Bruno *et al*. 1996), thus our interest in conserved elastic energies.

In this paper we develop and demonstrate a numerical method for evaluation of the overall elastic energy in polycrystals. This method is based on a rapidly convergent sequence of approximations which result as generalizations of a class of upper bounds introduced recently (Bruno *et al*. 1996; Smyshlyaev & Willis 1998). (The numerical calculations suggest that our new approximations are themselves upper bounds. We believe that this is in fact the case but we fall short of giving a rigorous argument to prove this assertion.) This numerical method is very fast indeed: it can resolve configurations containing millions of grains in computation times of the order of minutes on current desktop computers. Consideration of three-dimensional polycrystals, general microgeometries, geometric nonlinearities and arbitrary boundary conditions all fall within the scope of our methods. Together with improvements of various aspects of our algorithms (such as adaptive mesh refinement and high-order interpolation of the arrays of transformation strains), these additional applications will be left for future work.

This paper is organized as follows. In § 2 we describe the polycrystals we consider and we derive a variety of useful expressions for the effective energy. In § 3 we motivate and introduce a convergent series of approximations and we describe the numerical method that we use for their evaluation. These approximations reduce the complexity of our numerics from $\mathcal{O}(N^2)$ to $\mathcal{O}(N)$ operations, where N is the number of component crystallites. In §§ 4 and 5 we then specialize our results to a model polycrystal for which, in addition to our numerics, we derive rigorous upper

and lower bounds. In § 5, finally, we present numerical results, and we comment on the salient features of the effective energy and its bounds.

2. Elastic energy

Here we describe the polycrystals we consider, we introduce the effective energy and we derive a number of related identities that we will need in the rest of the paper. While this section follows closely § 2 of Bruno *et al.* (1996), we draw attention to the decomposition (2.19), (2.20) which plays a central role in our numerical methods and bounds. Our presentation is complete but brief (we refer to Bruno *et al.* (1996) and Smyshlyaev & Willis (1998) for a more detailed discussion).

(*a*) *Microgeometry and texture*

We consider two-dimensional polycrystals $\mathcal{P}$, consisting of a collection of grains or crystallites G:

$$\mathcal{P} = \bigcup_{G \in \mathcal{G}} G.$$

The crystallographic orientation of each grain G is given by an angle $\theta = \theta(G)$ $(0 \leqslant \theta < \frac{1}{2}\pi)$. We take both grains and orientations to be random variables, and we assume that their corresponding statistical distributions are spatially homogeneous. These are the same conditions assumed in Bruno *et al.* (1996) and we refer the reader to that paper for a more detailed discussion of the underlying statistics. As in Bruno *et al.* (1996), we assume in this paper the geometrically linear approximation.

Each grain can undergo a shape-deforming phase transition. We consider volume-preserving transformation strains, which are often found in practice. Without loss of generality we take the different basic transformation strains (or variants) in a single crystal of orientation $\theta = 0$ to be given by the matrices

$$\begin{bmatrix} a & 0 \\ 0 & -a \end{bmatrix} \quad \text{and} \quad \begin{bmatrix} -a & 0 \\ 0 & a \end{bmatrix}, \tag{2.1}$$

where a is a material constant. We then assume that the possible transformation strains $\varepsilon^{\mathrm{T}}(x)$ at a point x of such a crystal are the twin combinations of the strains in (2.1), that is

$$\varepsilon^{\mathrm{T}}(x) = \lambda(x) \begin{bmatrix} a & 0 \\ 0 & -a \end{bmatrix} \quad \text{with } -1 \leqslant \lambda(x) \leqslant 1. \tag{2.2}$$

As a consequence, if the orientation of a grain G is not 0 but $\theta = \theta(G)$, its possible transformations strains are

$$\varepsilon^{\mathrm{T}}(x) = \lambda(x) R \begin{bmatrix} a & 0 \\ 0 & -a \end{bmatrix} R^{\mathrm{T}} = \lambda(x) a \begin{bmatrix} \cos(2\theta) & \sin(2\theta) \\ \sin(2\theta) & -\cos(2\theta) \end{bmatrix}, \tag{2.3}$$

where $-1 \leqslant \lambda(x) \leqslant 1$ and R is the rotation by an angle θ:

$$R = \begin{bmatrix} \cos\theta & -\sin\theta \\ \sin\theta & \cos\theta \end{bmatrix}. \tag{2.4}$$

In accordance with our assumptions on the microstructure and texture, the set of admissible transformation strains is

$$\mathcal{S}^{\mathrm{T}} = \{\varepsilon^{\mathrm{T}} : \varepsilon^{\mathrm{T}} = \varepsilon^{\mathrm{T}}(x) \text{ is a statistically spatially homogeneous tensor of the form (2.3)}\}. \tag{2.5}$$

(*b*) *The homogenized energy*

As we said, our goal is to produce rigorous estimates and numerical computations of the homogenized energy of a polycrystal $\mathcal{P}$. Roughly speaking, the homogenized energy $\mathcal{E} = \mathcal{E}(\varepsilon^0)$, corresponding to a given (constant) applied strain ε^0 is the elastic energy under boundary conditions

$$u_i(x) = \varepsilon^0_{ij} x_j, \quad x \in \partial\mathcal{P} \tag{2.6}$$

for the displacement u_i, in the limit as the grain size tends to 0.

Given an assignment of transformation strains ε^{T}, the stress σ is given by

$$\sigma_{ij} = c_{ijk\ell}(u_{k,\ell} - \varepsilon^{\mathrm{T}}_{k\ell}), \tag{2.7}$$

where the displacement u satisfies equation (2.6) at the boundary of $\mathcal{P}$ as well as the equilibrium equations

$$\sigma_{ij,j} = 0. \tag{2.8}$$

Throughout this paper we assume isotropic stiffness,

$$c_{ijk\ell} = \frac{2\nu}{1-2\nu}\mu\delta_{ij}\delta_{k\ell} + \mu\delta_{ik}\delta_{j\ell} + \mu\delta_{i\ell}\delta_{jk},$$

with shear modulus μ and Poisson ratio ν, and we assume the elastic tensor of both phases to be identical. (The methods of this paper can be generalized to cases in which this restriction is not satisfied.)

To account for the smallness of the grains, we introduce the parameter β as the ratio between the diameter of a typical grain and the diameter of the polycrystal. The homogenized or effective energy $\mathcal{E}$ is given by the small-grain limit

$$\mathcal{E} = \lim_{\beta\to 0} \min_{\varepsilon^{\mathrm{T}}} \frac{1}{2|\mathcal{P}|} \int_{\mathcal{P}} \sigma_{ij}(u_{i,j} - \varepsilon^{\mathrm{T}}_{ij}), \tag{2.9}$$

where u satisfies (2.6)–(2.8). Thus, defining

$$W = W(\varepsilon^{\mathrm{T}}) = \lim_{\beta\to 0} \frac{1}{2|\mathcal{P}|} \int_{\mathcal{P}} \sigma_{ij}(u_{i,j} - \varepsilon^{\mathrm{T}}_{ij}) \tag{2.10}$$

and commuting the operations of limit and minimization in (2.9), we have (see Bruno *et al*. 1996)

$$\mathcal{E} = \min_{\varepsilon^{\mathrm{T}}} W(\varepsilon^{\mathrm{T}}). \tag{2.11}$$

We now proceed with the derivation of some useful relations for the energy W. We split the displacement u into three portions, $u = u^{(1)} + u^{(2)} + u^{(3)}$. Here $u^{(1)}$ equals the displacement that would be produced by the boundary conditions (2.6)

under a constant transformation strain $\varepsilon^{\mathrm{T}(1)}$ equal to the average of the given array of transformation strains

$$\varepsilon_{k\ell}^{\mathrm{T}(1)} = \varepsilon_{k\ell}^{\mathrm{T(av)}} = \lim_{\beta\to 0} \frac{1}{|\mathcal{P}|} \int_{\mathcal{P}} \varepsilon_{k\ell}^{\mathrm{T}} \,\mathrm{d}x. \tag{2.12}$$

This gives

$$u_i^{(1)} = \varepsilon_{ij}^0 x_j \tag{2.13}$$

and the associated stress

$$\sigma_{ij}^{(1)} = c_{ijk\ell}(u_{k,\ell}^{(1)} - \varepsilon_{k\ell}^{\mathrm{T(av)}}). \tag{2.14}$$

The displacement $u^{(2)}$, on the other hand, is the solution of the equations of elasticity in the plane under the transformation strain

$$\varepsilon_{k\ell}^{\mathrm{T}(2)}(x) = \begin{cases} \varepsilon_{k\ell}^{\mathrm{T}}(x) - \varepsilon_{k\ell}^{\mathrm{T(av)}}, & \text{if } x \in \mathcal{P}, \\ 0, & \text{otherwise,} \end{cases} \tag{2.15}$$

and vanishing boundary conditions at infinity. The corresponding stress is

$$\sigma_{ij}^{(2)} = \begin{cases} c_{ijk\ell}[u_{k,\ell}^{(2)} - (\varepsilon_{k\ell}^{\mathrm{T}} - \varepsilon_{k\ell}^{\mathrm{T(av)}})], & \text{if } x \in \mathcal{P}, \\ c_{ijk\ell} u_{k,\ell}^{(2)}, & \text{otherwise.} \end{cases} \tag{2.16}$$

Finally we define

$$u^{(3)} = u - u^{(1)} - u^{(2)} \quad \text{and} \quad \sigma_{ij}^{(3)} = c_{ijk\ell} u_{k,\ell}^{(3)}.$$

Following Bruno *et al.* (1996), it can be seen that $u^{(2)}$, $u^{(3)}$ and $\sigma^{(3)}$ tend to 0 strongly as the grain size tends to 0. In addition, we now note that

$$\lim_{\beta\to 0} \int_{\mathcal{P}} \sigma_{ij}^{(1)}[u_{i,j}^{(2)} - (\varepsilon_{ij}^{\mathrm{T}} - \varepsilon_{ij}^{\mathrm{T(av)}})] = 0. \tag{2.17}$$

(Indeed we have

$$(1) \quad \int_{\mathcal{P}} \sigma_{ij}^{(1)}(\varepsilon_{ij}^{\mathrm{T}} - \varepsilon_{ij}^{\mathrm{T(av)}}) \to 0,$$

since $\varepsilon_{ij}^{\mathrm{T}} - \varepsilon_{ij}^{\mathrm{T(av)}}$ tends to 0 weakly; and

$$(2) \quad \int_{\mathcal{P}} \sigma_{ij}^{(1)} u_{i,j}^{(2)} \to 0,$$

as it can be shown by integration by parts since $u^{(2)}$ tends to 0 strongly.) In view of these observations and calling

$$W_1 = \lim_{\beta\to 0} \frac{1}{2|\mathcal{P}|} \int_{\mathcal{P}} \sigma_{ij}^{(1)}[u_{i,j}^{(1)} - \varepsilon_{ij}^{\mathrm{T(av)}}], \tag{2.18}$$

$$W_2 = \lim_{\beta\to 0} \frac{1}{2|\mathcal{P}|} \int_{\mathcal{P}} \sigma_{ij}^{(2)}[u_{i,j}^{(2)} - (\varepsilon_{ij}^{\mathrm{T}} - \varepsilon_{ij}^{\mathrm{T(av)}})], \tag{2.19}$$

we finally obtain the expression

$$W = W_1 + W_2, \tag{2.20}$$

which gives the strain energy W as a sum of energies for two elasticity problems which are only coupled through the constant tensor $\varepsilon^{\mathrm{T(av)}}$.

(c) *Explicit expressions for W_1 and W_2*

In order to compute the upper bound and also for our numerical calculations, we will need explicit formulae for W_1 and W_2 as functions of the transformation strain ε^{T}. We describe these formulae next. In view of equations (2.13), (2.14) and (2.18) it follows that

$$W_1 = \tfrac{1}{2} c_{ijk\ell}(\varepsilon^0_{ij} - \varepsilon^{\mathrm{T(av)}}_{ij})(\varepsilon^0_{k\ell} - \varepsilon^{\mathrm{T(av)}}_{k\ell}). \tag{2.21}$$

Our treatment of the quantity W_2, on the other hand, requires consideration of Eshelby solutions. Following Eshelby (1957), the displacement that vanishes at ∞, and is produced by a transformation strain $\gamma^{\mathrm{T}} = \gamma^{\mathrm{T}}(x)$ in a domain I, is given by

$$u_r = -c_{tsk\ell}\biggl\{\int_I \Gamma_{rt,s}(x-x')\gamma^{\mathrm{T}}_{k\ell}(x')\,\mathrm{d}x'\biggr\}, \tag{2.22}$$

where Γ is the fundamental solution for the equations of elasticity in two dimensions:

$$\Gamma_{ij} = \frac{1}{8\pi(1-\nu)\mu}\biggl\{\frac{x_i x_j}{r^2} - (3-4\nu)\delta_{ij}\log(r)\biggr\}.$$

It follows that the displacement $u^{(2)}$ is given by

$$u^{(2)}_r = -c_{tsk\ell}\biggl\{\int_{\mathcal{P}} \Gamma_{rt,s}(x-x')(\varepsilon^{\mathrm{T}}_{k\ell}(x') - \varepsilon^{\mathrm{T(av)}}_{k\ell})\,\mathrm{d}x'\biggr\} \tag{2.23}$$

and, therefore, after some manipulations we obtain that W_2 can be rewritten as (see (2.19), (2.16) and (2.23))

$$\begin{aligned} W_2 = \frac{1}{2|\mathcal{P}|}c_{ijru}c_{tsk\ell}\int_{\mathcal{P}}(\varepsilon^{\mathrm{T}}_{ij}(x) - \varepsilon^{\mathrm{T(av)}}_{ij})\biggl\{\int_{\mathcal{P}}\Gamma_{rt,s}(x-x')(\varepsilon^{\mathrm{T}}_{k\ell}(x') - \varepsilon^{\mathrm{T(av)}}_{k\ell})\,\mathrm{d}x'\biggr\}_{,u}\,\mathrm{d}x \\ + \frac{1}{2|\mathcal{P}|}c_{ijk\ell}\int_{\mathcal{P}}(\varepsilon^{\mathrm{T}}_{ij}(x) - \varepsilon^{\mathrm{T(av)}}_{ij})(\varepsilon^{\mathrm{T}}_{k\ell}(x) - \varepsilon^{\mathrm{T(av)}}_{k\ell})\,\mathrm{d}x. \end{aligned} \tag{2.24}$$

3. Approximations and their numerical evaluations

After describing our discretization strategy in § 3 *a* we introduce, in § 3 *b*, a sequence of approximations for the effective energy. These approximations, which result from minimization of a related variational problem, can be evaluated with a reduced operation count: $\mathcal{O}(N)$ operations, where N is the number of grains. The minimization problem itself requires careful consideration; a discussion in this regard is given in § 3 *c*.

Since the effective energy does not depend on the shape of the sample, in what follows we assume the polycrystal occupies the square

$$\mathcal{P} = [0,1]\times[0,1]. \tag{3.1}$$

(a) *Discretization*

Given an integer m, we discretize the set $\mathcal{P}$ into $M = m^2$ elements E_{pq}, $0 \leqslant p, q \leqslant m-1$ of size $h = 1/m$. For simplicity, we take the discretizing elements themselves as squares:

$$E_{pq} = \boldsymbol{a}_{pq} + [0,h]\times[0,h], \quad \text{where } \boldsymbol{a}_{pq} = h\cdot(p,q); \tag{3.2}$$

an arbitrary shaped grain is thus approximated by a union of square elements. (Clearly, however, use of polygonal and polyhedral elements is more adequate in general applications.) We assign to each element E_{pq} the crystallographic orientation of the grain that contains it or, if the element intersects more than one grain, the orientation of the grain with which it has the largest intersection. The transformation strain ε^{T} is taken to be constant within each element; we use the notation $\varepsilon^{\mathrm{T}}_{ij}(E)$ for the value of the transformation strain within the element E.

Our discretization replaces the integrals over $\mathcal{P}$ in equation (2.24) by the sum of integrals over the elements $\{E_{pq}\}$. We thus obtain

$$\begin{aligned} W_2 \approx W_2^h = \sum_{E,F\subseteq\mathcal{P}} \frac{1}{2|\mathcal{P}|} c_{ijru}c_{tsk\ell}\left[\int_E \left\{\int_F \Gamma_{rt,s}(x-x')\,\mathrm{d}x'\right\}_{,u}\mathrm{d}x\right] \\ \times (\varepsilon^{\mathrm{T}}_{ij}(E)-\varepsilon^{\mathrm{T(av)}}_{ij})(\varepsilon^{\mathrm{T}}_{k\ell}(F)-\varepsilon^{\mathrm{T(av)}}_{k\ell}) \\ + \sum_{E\subseteq\mathcal{P}} \frac{1}{2|\mathcal{P}|} c_{ijk\ell}|E|(\varepsilon^{\mathrm{T}}_{ij}(E)-\varepsilon^{\mathrm{T(av)}}_{ij})(\varepsilon^{\mathrm{T}}_{k\ell}(E)-\varepsilon^{\mathrm{T(av)}}_{k\ell}), \end{aligned} \tag{3.3}$$

where the summation is performed over all pairs of elements E and F contained in the polycrystal $\mathcal{P}$. Since the integrals in (3.3) can be computed analytically (see Appendix A), W_2^h can be evaluated explicitly. After introduction of the strain deviators d_1^{T} and d_2^{T},

$$d_1^{\mathrm{T}}(E) = \varepsilon^{\mathrm{T}}_{11}(E) = -\varepsilon^{\mathrm{T}}_{22}(E) \quad \text{and} \quad d_2^{\mathrm{T}}(E) = \varepsilon^{\mathrm{T}}_{12}(E) = \varepsilon^{\mathrm{T}}_{21}(E) \tag{3.4}$$

(which determine completely the volume preserving strain ε^{T}), their averages

$$d_i^{\mathrm{T(av)}} = \frac{1}{|\mathcal{P}|}\int_{\mathcal{P}} d_i^{\mathrm{T}}(x)\,\mathrm{d}x = \frac{1}{|\mathcal{P}|}\sum_{E\subseteq\mathcal{P}} |E| d_i^{\mathrm{T}}(E), \tag{3.5}$$

and certain explicit constants a_{ij}^{EF} given in Appendix A, equation (3.3) becomes

$$W_2^h = \mu \sum_{E,F\subseteq\mathcal{P}} a_{ij}^{EF}(d_i^{\mathrm{T}}(E)-d_i^{\mathrm{T(av)}})(d_j^{\mathrm{T}}(F)-d_j^{\mathrm{T(av)}}). \tag{3.6}$$

The expression (2.21) for W_1 is in closed form and does not require discretization. Writing the applied strain as

$$\varepsilon^0 = \begin{bmatrix} h^0+d_1^0 & d_2^0 \\ d_2^0 & h^0-d_1^0 \end{bmatrix}, \tag{3.7}$$

and using the deviators of the transformation strain, W_1 can be rewritten as

$$W_1 = \frac{2\mu}{1-2\nu}(h^0)^2 + 2\mu[(d_1^0-d_1^{\mathrm{T(av)}})^2 + (d_2^0-d_2^{\mathrm{T(av)}})^2]. \tag{3.8}$$

(*b*) *Truncation of* W_2^h

We now introduce a sequence of approximations for the quantity W_2^h of equation (3.6), which, while maintaining accuracy, will allow us to reduce substantially the complexity of our minimization problem. These truncations depend on the statistics of the underlying field of crystallographic orientations and they can be used in a variety of contexts; a concrete application is given in § 5.

Our truncations are motivated by the analysis in Bruno *et al.* (1996) leading to upper bounds on the overall energy. In that paper bounds were obtained via minimization of the energy integral over a restricted set $\mathcal{T}$ of transformation strains defined by

$$\mathcal{T} = \{\varepsilon^{\mathrm{T}}(x) : \varepsilon^{\mathrm{T}} \text{ is admissible and } \varepsilon^{\mathrm{T}}(x) \text{ is uncorrelated from } \varepsilon^{\mathrm{T}}(y) \text{ whenever } x \text{ and } y \text{ belong to different grains}\}. \quad (3.9)$$

The significance of the conditions defining the set $\mathcal{T}$ becomes apparent as we average W_2^h given by the expression (3.6) over the statistical ensemble to obtain

$$\langle W_2^h \rangle = \mu \sum_{E,F \subseteq \mathcal{P}} a_{ij}^{EF} \langle (d_i^{\mathrm{T}}(E) - d_i^{\mathrm{T(av)}})(d_j^{\mathrm{T}}(F) - d_j^{\mathrm{T(av)}}) \rangle. \quad (3.10)$$

For an element in $\mathcal{T}$, equation (3.10) simplifies to

$$\langle W_2^h \rangle = \mu \sum_{\substack{E,F \subseteq \mathcal{P} \\ E,F \text{ in the same grain}}} a_{ij}^{EF} \langle (d_i^{\mathrm{T}}(E) - d_i^{\mathrm{T(av)}})(d_j^{\mathrm{T}}(F) - d_j^{\mathrm{T(av)}}) \rangle, \quad (3.11)$$

since by the assumed uncorrelation we have

$$\langle (d_i^{\mathrm{T}}(E) - d_i^{\mathrm{T(av)}})(d_j^{\mathrm{T}}(F) - d_j^{\mathrm{T(av)}}) \rangle = \langle d_i^{\mathrm{T}}(E) - d_i^{\mathrm{T(av)}} \rangle \langle d_j^{\mathrm{T}}(F) - d_j^{\mathrm{T(av)}} \rangle = 0 \quad (3.12)$$

whenever E and F lie in different grains. (To obtain the last equality we have used the fact that $\langle \varepsilon \rangle = \varepsilon^{\mathrm{T(av)}}$ since ε^{T} is statistically spatially homogeneous.)

The bounds obtained through this process are in fact very good estimates (Bruno *et al.* 1996; Smyshlyaev & Willis 1998); here we seek to extend these ideas to produce a convergent sequence of approximations. To do this we need to take into account the fact that the minimizing distribution of transformation strains leads to correlations between transformation strains of different grains. This observation leads us to our improved approximations.

Defining the separation between two elements E and F as the distance between the grains that contain them and choosing a fixed non-negative integer r, our approximation consists of neglecting the contribution of the pair E, F to the sum (3.11) whenever the separation $\mathrm{sep}(E,F)$ between the elements E and F is greater than or equal to r. The resulting approximation, denoted by $W_2^{h,r}$, is thus given by (cf. equation (3.11))

$$W_2^h \approx W_2^{h,r} = \mu \sum_{\substack{E,F \subseteq \mathcal{P} \\ \mathrm{sep}(E,F) < r}} a_{ij}^{EF} (d_i^{\mathrm{T}}(E) - d_i^{\mathrm{T(av)}})(d_j^{\mathrm{T}}(F) - d_j^{\mathrm{T(av)}}). \quad (3.13)$$

The complete approximation to the energy is therefore given by

$$W \approx W^{h,r} = W_1 + W_2^{h,r}. \quad (3.14)$$

(*c*) *Minimization*

The deviators d_1^{T} and d_2^{T} are related. Indeed, denoting by $\theta(E)$ the orientation of the element E, the deviators can be written in the form

$$d_1^{\mathrm{T}}(E) = a\lambda(E)\cos(2\theta(E)) \quad \text{and} \quad d_2^{\mathrm{T}}(E) = a\lambda(E)\sin(2\theta(E)) \quad (3.15)$$

for some number $\lambda(E)$ with $-1 \leqslant \lambda(E) \leqslant 1$ (see (2.3)). Thus, the strain energy and its approximation $W^{h,r}$ are functions of the array $[\lambda_{ij}]$ formed by the parameters $\lambda(E)$ for all the discretization elements E:

$$\lambda_{ij} = \lambda(E_{ij}).$$

Numerical evaluation of the effective energy (2.3) then results via solution of the minimization problem

$$\mathcal{E}^{h,r} = \min\{W^{h,r}([\lambda_{ij}]) : -1 \leqslant \lambda_{ij} \leqslant 1\}. \tag{3.16}$$

This is a quadratic programming problem for $[\lambda_{ij}]$ since $W^{h,r}$ is a convex quadratic function and the set of admissible variables is a convex polygon. Many different algorithms can be found in the literature for the solution of this class of problems, and the best choice for our purposes depends on the characteristics of the polycrystal under consideration. Our discussion on the explicit evaluation of the homogenized energy $\mathcal{E}$ will therefore be postponed until § 5, where we restrict our attention to a particular class of polycrystals. There we describe our minimization strategies, we study the convergence and complexity of our method and we comment on possible extensions to different classes of polycrystals.

4. Upper and lower bounds: a test case

In addition to numerical calculations it is valuable to consider rigorous upper and lower bounds for the energy, as they provide a degree of validation for the numerics, and they constitute a source of useful intuition on the problem. (In this regard we note, for example, that the numerical method we are presently proposing resulted as a generalization of the upper bounds of Bruno *et al*. (1996) and Smyshlyaev & Willis (1998).)

The discussion in the previous sections has been general: it applies to arbitrary polycrystals as described in § 2. In what follows we restrict our attention to a particular case in which (1) the crystallographic orientation of the grains is a random variable with uniform probability distribution; (2) the parameter λ of equation (2.3) is constant within each grain; and (3) the polycrystal $\mathcal{P}$ consists of $N = n^2$ square grains of the same size. Grains will be labelled so that the (i, j)th grain is given by

$$G_{ij} = \boldsymbol{g}_{ij} + [0, 1/n]^2, \quad \text{where } \boldsymbol{g}_{ij} = (i, j)/n, \tag{4.1}$$

and our polycrystal is then

$$\mathcal{P} = \bigcup_{0 \leqslant i,j \leqslant n-1} G_{ij} = [0, 1]^2. \tag{4.2}$$

The microgeometrical assumptions (1) and (3) require no comments. With regards to condition (2), we note that small-grained polycrystals lead frequently to singly or multiply twinned martensites in each grain, which are well described by such constant values of λ (cf., for example, Arlt 1990). Other intragranular microgeometries do occur in practice, however. Application of our methods to such cases are not pursued in this paper (see Bhattacharya & Kohn (1997) for bounds applicable to completely unrestrained intragranular microstructures in the small applied-strain regime). The types of intragranular microgeometries allowed in numerical calculations or bounds

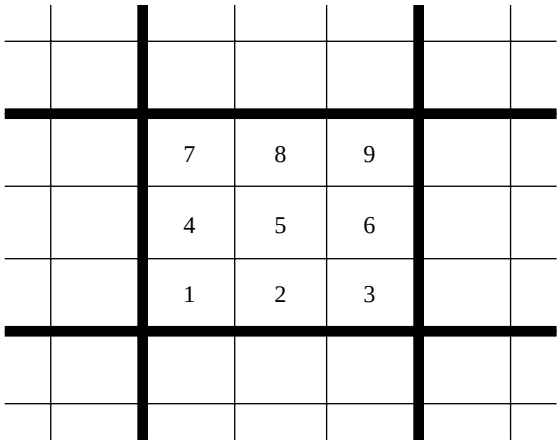

Figure 1. A group of grains in the lower-bound decomposition of $\mathcal{P}$; $n_{\mathrm{g}} = 3$.

must reflect the microgeometric characteristics of the polycrystal being modelled. In reflecting such geometric features the present energetic framework can account, in fact, for physical effects which are not a consequence of the energetic framework itself—such as dissipation, atomic-level energy barriers, etc.

Our derivation of lower bounds in § 4 *a* is based on a new approach. The upper bound of § 4 *b*, on the other hand, follows from the methods of Bruno *et al.* (1996) (see also Smyshlyaev & Willis (1998) for generalization to arbitrary rotationally symmetric microgeometries and improved optimization procedures). The results of § 4 *b* further extend these methods to the non-rotationally symmetric case presently under consideration.

(*a*) *Lower bound*

(i) *Lower bounds for small applied strains*

Our derivation of lower bounds is based on partition of the polycrystal into a number of *groups of grains*. We thus divide the polycrystal $\mathcal{P}$ of equation (4.2) into groups containing $N_{\mathrm{g}} = n_{\mathrm{g}}^2$ grains. The total number of grains in the polycrystal may not be divisible by N_{g}, but we can always cover almost all of the polycrystal's body by using such groups. More specifically, we write

$$\mathcal{P} \supseteq \bigcup_{A \in \mathcal{A}} A, \tag{4.3}$$

where, calling

$$A_{n_1 n_2} = \bigcup_{i=n_1 n_{\mathrm{g}}}^{(n_1+1)n_{\mathrm{g}}-1} \; \bigcup_{j=n_2 n_{\mathrm{g}}}^{(n_2+1)n_{\mathrm{g}}-1} G_{ij}, \tag{4.4}$$

we have set (see figure 1)

$$\mathcal{A} = \{A_{n_1 n_2} : 0 \leqslant n_1,\ n_2 \leqslant (n-1)/n_{\mathrm{g}}\}. \tag{4.5}$$

From equation (2.19) and denoting, for $A \in \mathcal{A}$

$$W_A = \frac{1}{2|A|}\int_A \sigma_{ij}^{(2)}[u_{ij}^{(2)} - (\varepsilon_{ij}^{\mathrm{T}} - \varepsilon_{ij}^{\mathrm{T(av)}})], \tag{4.6}$$

we evidently have

$$W_2 \geqslant \sum_{A\in\mathcal{A}} |A| W_A. \tag{4.7}$$

Now, the quantities W_A themselves can be bounded from below by the energy of a corresponding traction-free boundary-value problem. Indeed, let $\tilde{v}$ be the solution of the equations

$$\left.\begin{aligned} \tau_{ij,j} &= 0, \\ \tau_{ij} &= c_{ijk\ell}[\tilde{v}_{k,\ell} - (\varepsilon_{k\ell}^{\mathrm{T}} - \varepsilon_{k\ell}^{\mathrm{T(av)}})], \\ \tau_{ij}(x)\hat{n}_j(x) &= 0, \quad x \in \partial A, \end{aligned}\right\} \tag{4.8}$$

where $\hat{n}$ is the normal to the boundary of A. Then, defining

$$F_A = \frac{1}{2|A|}\int_A \tau_{ij}[\tilde{v}_{i,j} - (\varepsilon_{ij}^{\mathrm{T}} - \varepsilon_{ij}^{\mathrm{T(av)}})], \tag{4.9}$$

we have

$$W_A \geqslant F_A, \tag{4.10}$$

since the solution of the traction-free problem minimizes the corresponding energy integral. These expressions may be simplified somewhat: in terms of the displacement field

$$v_i(x) = \tilde{v}_i(x) + \varepsilon_{ij}^{\mathrm{T(av)}} x_j,$$

which solves the equations

$$\left.\begin{aligned} \tau_{ij,j} &= 0, \\ \tau_{ij} &= c_{ijk\ell}(v_{k,\ell} - \varepsilon_{k\ell}^{\mathrm{T}}), \\ \tau_{ij}(x)\hat{n}_j(x) &= 0, \quad x \in \partial A, \end{aligned}\right\} \tag{4.11}$$

the expression for F_A is made to read

$$F_A = \frac{1}{2|A|}\int_A \tau_{ij}(v_{i,j} - \varepsilon_{ij}^{\mathrm{T}}). \tag{4.12}$$

From equations (4.7) and (4.10) we obtain the estimate

$$W = W_1 + W_2 \geqslant W_1 + \sum_{A\in\mathcal{A}} |A| F_A; \tag{4.13}$$

our lower bound will result as the minimum value of the right-hand side of equation (4.13). As we will see the value of this minimum does not change if the minimization set is restricted to arrays of transformation strains whose values within each group depend solely on the crystallographic orientations in the group.

To demonstrate this and to derive our lower bound we introduce some notation: in what follows we use the integers $1, 2, \ldots, N_{\mathrm{g}}$ to number the N_{g} grains within each group $A \in \mathcal{A}$ (as indicated in figure 1). In addition, we denote the orientation and transformation strain of the ith grain of a given group A by $\theta_i = \theta_i(A)$ and $\varepsilon^{\mathrm{T}(i)} = \varepsilon^{\mathrm{T}(i)}(A)$, respectively. From equation (2.3), finally, the transformation strain $\varepsilon^{\mathrm{T}(i)}$ is given by

$$\varepsilon^{\mathrm{T}(i)} = a\lambda_i \begin{bmatrix} \cos(2\theta_i) & \sin(2\theta_i) \\ \sin(2\theta_i) & -\cos(2\theta_i) \end{bmatrix} \tag{4.14}$$

for some number $\lambda_i = \lambda_i(A)$ with

$$-1 \leqslant \lambda_i \leqslant 1.$$

In connection with our minimization problem, we note that the quantity F_A depends on the transformation strains of grains within the group A only. From the representation (4.14) it follows that F_A can be viewed as a function of the $2N_{\mathrm{g}}$ variables $\boldsymbol{\theta} = \boldsymbol{\theta}(A) = (\theta_1(A), \ldots, \theta_{N_{\mathrm{g}}}(A))$ and $\boldsymbol{\lambda} = \boldsymbol{\lambda}(A) = (\lambda_1(A), \ldots, \lambda_{N_{\mathrm{g}}}(A))$:

$$F_A = F(\boldsymbol{\lambda}, \boldsymbol{\theta}). \tag{4.15}$$

To show that minimization of the right-hand side of (4.13) is indeed equivalent to its minimization over the restricted set of transformation strains in which $\boldsymbol{\lambda}$ depends on $\boldsymbol{\theta}$, we argue as follows. We define

$$\mathcal{B}(\boldsymbol{\theta}) = \{A : A \in \mathcal{A} \text{ and } \boldsymbol{\theta} \leqslant \boldsymbol{\theta}(A) \leqslant \boldsymbol{\theta} + \mathrm{d}\boldsymbol{\theta}\}. \tag{4.16}$$

Since F is a positive quadratic function, and therefore a convex function of $\boldsymbol{\lambda}$, for every pair A_1, A_2 of elements of $\mathcal{B}(\boldsymbol{\theta})$ we obtain

$$F_{A_1} + F_{A_2} = F(\boldsymbol{\lambda}(A_1), \boldsymbol{\theta}) + F(\boldsymbol{\lambda}(A_2), \boldsymbol{\theta}) \geqslant 2F(\tfrac{1}{2}(\boldsymbol{\lambda}(A_1) + \boldsymbol{\lambda}(A_2)), \boldsymbol{\theta}) + \mathcal{O}(\mathrm{d}\theta).$$

Thus, defining

$$\boldsymbol{\lambda} = \boldsymbol{\lambda}(\boldsymbol{\theta}) = \frac{1}{\#(\mathcal{B}(\boldsymbol{\theta}))} \sum_{A \in \mathcal{B}(\boldsymbol{\theta})} \boldsymbol{\lambda}(A), \tag{4.17}$$

we have

$$\sum_{A \in \mathcal{B}(\boldsymbol{\theta})} F_A \geqslant \#(\mathcal{B}(\boldsymbol{\theta})) F(\boldsymbol{\lambda}(\boldsymbol{\theta}), \boldsymbol{\theta}). \tag{4.18}$$

Clearly, in view of our assumption on the texture of the polycrystal (point (2) in the introduction to § 4), we have

$$|A| \cdot \#(\mathcal{B}) = (2/\pi)^{N_{\mathrm{g}}}\, \mathrm{d}\theta_1 \cdots \mathrm{d}\theta_{N_{\mathrm{g}}},$$

so that, multiplying equation (4.18) by $|A|$ and adding over $\boldsymbol{\theta}$, we obtain

$$\sum_{A \in \mathcal{A}} |A| F_A \geqslant (2/\pi)^{N_{\mathrm{g}}} \int_{[0,\pi/2]^{N_{\mathrm{g}}}} F(\boldsymbol{\lambda}(\boldsymbol{\theta}), \boldsymbol{\theta})\, \mathrm{d}\theta_1 \cdots \mathrm{d}\theta_{N_{\mathrm{g}}}, \tag{4.19}$$

which shows that the restriction $\boldsymbol{\lambda} = \boldsymbol{\lambda}(\boldsymbol{\theta})$ does not change the value of the minimum, as claimed.

With regards to the first term of (4.13), on the other hand, it is easy to check that

$$\left.\begin{aligned} d_1^{\mathrm{T(av)}} &= \left(\frac{2}{\pi}\right)^{N_\mathrm{g}} \frac{a}{N_\mathrm{g}} \sum_{j=1}^{N_\mathrm{g}} \int_{[0,\pi/2]^{N_\mathrm{g}}} \lambda_j(\boldsymbol{\theta}) \cos(2\theta_j)\, \mathrm{d}\theta_1 \cdots \mathrm{d}\theta_{N_\mathrm{g}}, \\ d_2^{\mathrm{T(av)}} &= \left(\frac{2}{\pi}\right)^{N_\mathrm{g}} \frac{a}{N_\mathrm{g}} \sum_{j=1}^{N_\mathrm{g}} \int_{[0,\pi/2]^{N_\mathrm{g}}} \lambda_j(\boldsymbol{\theta}) \sin(2\theta_j)\, \mathrm{d}\theta_1 \cdots \mathrm{d}\theta_{N_\mathrm{g}}. \end{aligned}\right\} \tag{4.20}$$

It now follows from (3.8), (4.13) and (4.19) that

$$W = W_1 + W_2 \geqslant \mathcal{L}, \tag{4.21}$$

where

$$\mathcal{L} = \frac{2\mu}{1-2\nu}(h^0)^2 + 2\mu[(d_1^0 - d_1^{\mathrm{T(av)}})^2 + (d_2^0 - d_2^{\mathrm{T(av)}})^2] + \left(\frac{2}{\pi}\right)^{N_\mathrm{g}} \int_{[0,\pi/2]^{N_\mathrm{g}}} F(\boldsymbol{\lambda}(\boldsymbol{\theta}), \boldsymbol{\theta})\, \mathrm{d}\theta_1 \cdots \mathrm{d}\theta_{N_\mathrm{g}}. \tag{4.22}$$

Finally, minimizing $\mathcal{L}$ over *all* vector functions $\boldsymbol{\lambda} = \boldsymbol{\lambda}(\boldsymbol{\theta})$ we obtain our lower bound

$$L_1 = L_1(\varepsilon^0) = \min_{\boldsymbol{\lambda}} \mathcal{L}. \tag{4.23}$$

(We remark that we have not taken the minimization in (4.23) to be restricted to the set of functions $\boldsymbol{\lambda}$ satisfying $|\lambda_i(\boldsymbol{\theta})| \leqslant 1$. For large applied strains, this additional restriction would have provided a tighter lower bound than the one we obtain. We have avoided this extremely cumbersome computation and have contented ourselves by using a well-known elementary lower bound which, for such large applied strains, is itself rather tight (see § 4 *a* (ii)).) An explicit evaluation of our lower bounds is given in Appendix B, where we obtain the expression

$$L_1 = \frac{2\mu}{1-2\nu}(h^0)^2 + \mu(c_1(d_1^0)^2 + c_2(d_2^0)^2) \tag{4.24}$$

for certain constants c_1 and c_2. As it is clear from our analysis, these constants depend on the number N_g of grains within each group. Numerical values of the constants c_1 and c_2 for various values of $n_\mathrm{g} = \sqrt{N_\mathrm{g}}$ are given in table 1; comparisons of the resulting lower bounds with an upper bound and numerical evaluations of the energy are given in § 5.

(ii) *Lower bound for large applied strains*

As mentioned above, for large values of the applied strains it is advantageous to use an elementary lower bound. Such a bound can be obtained by neglecting the positive quantity W_2 in the expression (2.20) prior to the minimization (2.11):

$$\mathcal{E} \geqslant \min_{\varepsilon^\mathrm{T}} W_1. \tag{4.25}$$

(This expression is identical to the well-known result which is obtained from relaxation of the constraint of compatibility between grains. Indeed, W_2 can be made to

vanish by using appropriate *discontinuous* displacements.) From equation (3.8),

$$W_1 = \frac{2\mu}{1-2\nu}(h^0)^2 + 2\mu[(d_1^0 - d_1^{\mathrm{T(av)}})^2 + (d_2^0 - d_2^{\mathrm{T(av)}})^2], \tag{4.26}$$

we see that the minimum in (4.25) can in fact be obtained via minimization over the scalar variables $d_1^{\mathrm{T(av)}}$, $d_2^{\mathrm{T(av)}}$. To determine the range of possible values of these variables we use complex notation and we write, for an arbitrary x (see (2.3)),

$$d^{\mathrm{T(av)}}\mathrm{e}^{2\mathrm{i}\theta^{(av)}} = d_1^{\mathrm{T(av)}} + \mathrm{i}d_2^{\mathrm{T(av)}} = a\langle\lambda(x)\mathrm{e}^{2\mathrm{i}\theta(x)}\rangle.$$

Since $d^{\mathrm{T(av)}}$ is a real number, we may write, alternatively,

$$d^{\mathrm{T(av)}} = a\langle\lambda(x)\mathrm{e}^{2\mathrm{i}(\theta(x)-\theta^{(av)})}\rangle = a\langle\lambda(x)\cos(2(\theta(x)-\theta^{(av)}))\rangle.$$

Since the $\lambda(x)$ is only constrained by the inequality $|\lambda(x)| \leqslant 1$, we obtain

$$0 \leqslant d^{\mathrm{T(av)}} \leqslant a\langle|\cos(2(\theta(x)-\theta^{(av)}))|\rangle,$$

from which it follows that the quantity $(d_1^{\mathrm{T(av)}}, d_2^{\mathrm{T(av)}})$ may take values in the disc

$$(d_1^{\mathrm{T(av)}})^2 + (d_2^{\mathrm{T(av)}})^2 \leqslant \frac{4}{\pi^2}a^2. \tag{4.27}$$

Using the notation

$$(d^0)^2 = (d_1^0)^2 + (d_2^0)^2,$$

minimization of (4.26) over the set (4.27) finally yields the bound

$$\mathcal{E} \geqslant L_2, \quad \text{where } L_2 = \begin{cases} \dfrac{2\mu}{1-2\nu}(h^0)^2, & \text{if } 0 \leqslant d^0 \leqslant a\dfrac{2}{\pi}, \\ \dfrac{2\mu}{1-2\nu}(h^0)^2 + 2\mu\left(d^0 - a\dfrac{2}{\pi}\right)^2, & \text{if } d^0 \geqslant a\dfrac{2}{\pi}. \end{cases} \tag{4.28}$$

(*b*) *Upper bound*

We obtain an upper bound U through minimization of the energy over an 'uncorrelated' subset $\mathcal{T}$ of $\mathcal{S}^{\mathrm{T}}$ (see Bruno *et al.* 1996). Our arguments follow Bruno *et al.* (1996) and Smyshlyaev & Willis (1998); the details of our calculations are not identical to the previous ones since the microgeometry we consider does not satisfy the hypothesis of circular symmetry of Smyshlyaev & Willis (1998). We will be brief and we refer the reader to Bruno *et al.* (1996) and Smyshlyaev & Willis (1998) for a more detailed presentation.

Explicitly, we seek to minimize the energy over the set (see (2.5))

$$\mathcal{T} = \{\varepsilon^{\mathrm{T}} \in \mathcal{S}^{\mathrm{T}} : \varepsilon^{\mathrm{T}}(x) \text{ depends only on the orientation } \theta \text{ of the grain containing } x\}, \tag{4.29}$$

so that our upper bound is

$$U = \min_{\varepsilon^{\mathrm{T}} \in \mathcal{T}} W. \tag{4.30}$$

By ergodicity, the strain energy W does not depend on the particular realization under consideration; averaging over the ensemble of all possible realizations and minimizing over $\mathcal{T}$ we thus obtain

$$U = \min_{\varepsilon^{\mathrm{T}} \in \mathcal{T}} W = \min_{\varepsilon^{\mathrm{T}} \in \mathcal{T}} \langle W \rangle. \tag{4.31}$$

In the test case considered presently, as described in the introduction to § 4, the same arguments of § 3 (but with the grains playing the role of the elements) leads to (see (2.20), (3.8) and (3.6))

$$W = \langle W \rangle = \lim_{\beta \to 0} \Bigg\{ \frac{2\mu}{1-2\nu} (h^0)^2 + 2\mu[(d_1^0 - d_1^{\mathrm{T(av)}})^2 + (d_2^0 - d_2^{\mathrm{T(av)}})^2] + \mu \sum_{\{G,H \in \mathcal{G}: G,H \subseteq \mathcal{P}\}} a_{ij}^{GH} \langle (d_i^{\mathrm{T}}(G) - d_i^{\mathrm{T(av)}})(d_j^{\mathrm{T}}(H) - d_j^{\mathrm{T(av)}}) \rangle \Bigg\}. \tag{4.32}$$

Note that for any $\varepsilon^{\mathrm{T}} \in \mathcal{T}$, the transformation strains $\varepsilon^{\mathrm{T}}(x)$ and $\varepsilon^{\mathrm{T}}(y)$ are statistically independent whenever x and y lie within different grains. Thus, for different grains G and H we have

$$\langle (d_i^{\mathrm{T}}(G) - d_i^{\mathrm{T(av)}})(d_j^{\mathrm{T}}(H) - d_j^{\mathrm{T(av)}}) \rangle = \langle d_i^{\mathrm{T}}(G) - d_i^{\mathrm{T(av)}} \rangle \langle d_j^{\mathrm{T}}(H) - d_j^{\mathrm{T(av)}} \rangle = 0; \tag{4.33}$$

the last equality results from $\langle \varepsilon \rangle = \varepsilon^{\mathrm{T(av)}}$.

In view of our assumed uniform distribution of orientations, on the other hand, we obtain the relations

$$\langle (d_i^{\mathrm{T}}(G) - d_i^{\mathrm{T(av)}})(d_j^{\mathrm{T}}(G) - d_j^{\mathrm{T(av)}}) \rangle = \frac{2}{\pi} \int_0^{\pi/2} (d_i^{\mathrm{T}}(\theta) - d_i^{\mathrm{T(av)}})(d_j^{\mathrm{T}}(\theta) - d_j^{\mathrm{T(av)}}) \, \mathrm{d}\theta \tag{4.34}$$

for the diagonal terms in (4.32) and

$$d_i^{\mathrm{T(av)}} = \frac{2}{\pi} \int_0^{\pi/2} d_i^{\mathrm{T}}(\theta) \, \mathrm{d}\theta \tag{4.35}$$

for the average deviators. Here

$$d_i^{\mathrm{T}}(\theta) = d_i^{\mathrm{T}}(G), \quad i = 1, 2,$$

where $\theta = \theta(G)$ denotes the orientation of the grain G (cf. (4.29)).

To complete our evaluation of $W = \langle W \rangle$ we need the diagonal coefficients a_{ij}^{GG}. Explicit expressions for these quantities are given in Appendix A. Using those values together with equations (4.32)–(4.34) we obtain the following expression for the strain energy W—which is valid for an arbitrary $\varepsilon^{\mathrm{T}} \in \mathcal{T}$:

$$\begin{aligned} W = {} & \frac{2\mu}{1-2\nu} (h^0)^2 + 2\mu[(d_1^0 - d_1^{\mathrm{T(av)}})^2 + (d_2^0 - d_2^{\mathrm{T(av)}})^2] \\ & + \frac{\mu}{(1-\nu)} \left[1 - \frac{\log(4)}{\pi} \right] \left[\frac{2}{\pi} \int_0^{\pi/2} (d_1^{\mathrm{T}}(\theta))^2 \, \mathrm{d}\theta - (d_1^{\mathrm{T(av)}})^2 \right] \\ & + \mu \frac{\log(4)}{\pi(1-\nu)} \left[\frac{2}{\pi} \int_0^{\pi/2} (d_2^{\mathrm{T}}(\theta))^2 \, \mathrm{d}\theta - (d_2^{\mathrm{T(av)}})^2 \right]. \end{aligned} \tag{4.36}$$

For $\varepsilon^{\mathrm{T}} \in \mathcal{T}$ the deviator relations (2.3) define a quantity $\lambda = \lambda(\theta)$ as

$$d_1^{\mathrm{T}}(\theta) = a\lambda(\theta)\cos(2\theta) \quad \text{and} \quad d_2^{\mathrm{T}}(\theta) = a\lambda(\theta)\sin(2\theta). \tag{4.37}$$

The computation of the upper bound U now reduces to minimization of (4.36)—with the relations (4.37) and (4.35)—over the set of functions $\lambda = \lambda(\theta)$ satisfying $|\lambda(\theta)| \leqslant 1$ for all θ. This calculation is completed in Appendix C. Comparison of these results with our lower bounds and numerical calculations is given in § 5.

5. Results

In this section we present our numerical results and bounds. We thus discuss the characteristics of the energy curves and we present a detailed description of our numerical method and its convergence properties in the test case under consideration, as described in § 4. As it happens, numerical results, bounds and convergence tests are fully consistent with each other, and they demonstrate the robustness of our numerical approach.

In figures 2–5 and tables 1–5 we display various quantities related to the homogenized energy of the polycrystal of § 4 as functions of the magnitude ε of a deviatoric applied strain. We consider the computed values of the homogenized energy $\mathcal{E}$ itself, our upper and lower bounds U, and L, and, for reference, the 'austenite energy' E_{A}

$$E_{\mathrm{A}} = \tfrac{1}{2} c_{ijk\ell}\varepsilon^0_{ij}\varepsilon^0_{k\ell},$$

which equals the energy that would be required to deform the polycrystal in the absence of phase transitions. For definiteness (and following Bruno *et al.* (1996) and Smyshlyaev & Willis (1998)) we use the values $\mu = 100$ GPa, $\nu = 0.25$ and $a = 0.02$ for the elastic constants and the magnitude of the transformation strain (see (2.1)). In what follows, the size of the applied strain is characterized by a parameter ε through

$$\varepsilon^0 = \varepsilon \begin{bmatrix} 1 & 0 \\ 0 & -1 \end{bmatrix}. \tag{5.1}$$

The range $0 \leqslant \varepsilon \leqslant 0.04$ which we consider gives applied deviators covering the interesting domain in which most of the phase transitions occur. Consideration of applied strains containing hydrostatic components is not necessary, since such components decouple and lead to results which follow directly from the ones we present (see equations (3.6), (3.8)). Further, our numerics indicate that the polycrystal is effectively isotropic—although the microgeometry certainly is not—so that consideration of other applied shears is also unnecessary. This is clearly demonstrated in figure 2, where the calculated energy for applied strains of the form

$$\varepsilon^0(\theta) = R(\theta) \begin{bmatrix} 0.005 & 0 \\ 0 & -0.005 \end{bmatrix} R^{\mathrm{T}}(\theta) \tag{5.2}$$

is presented as a function of θ. (Here R is the rotation by an angle θ (see (2.4)).)

(*a*) *Homogenized energy*

Let us consider the computed values for the homogenized energy $\mathcal{E} = \mathcal{E}(\varepsilon)$ in figure 3. Consideration of these values shows two main ranges of quadratic behaviour

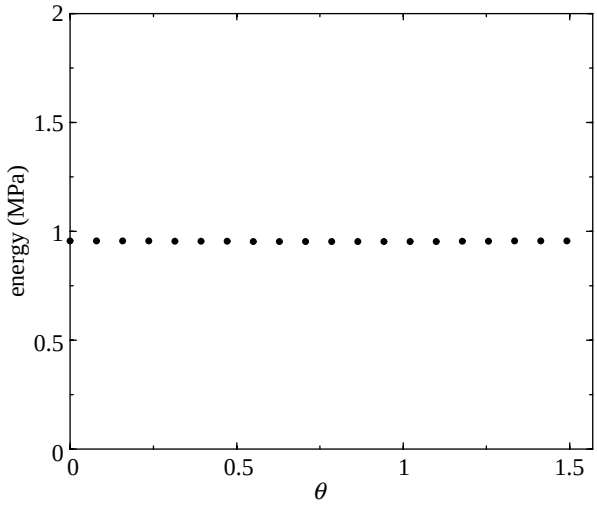

Figure 2. Energy corresponding to the applied strain $\varepsilon^0(\theta)$ of equation (5.2) as a function of θ.

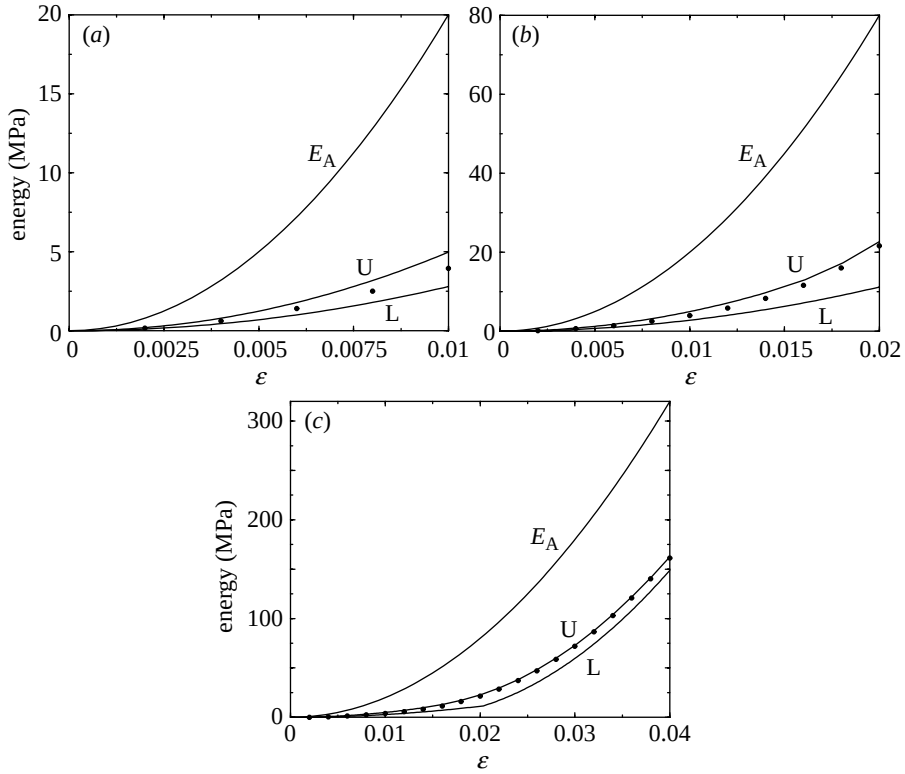

Figure 3. Austenite energy E_A, upper bound U, lower bound L and effective energy $\mathcal{E}$ (in dotted line) as functions of the parameter ε of equation (5.1).

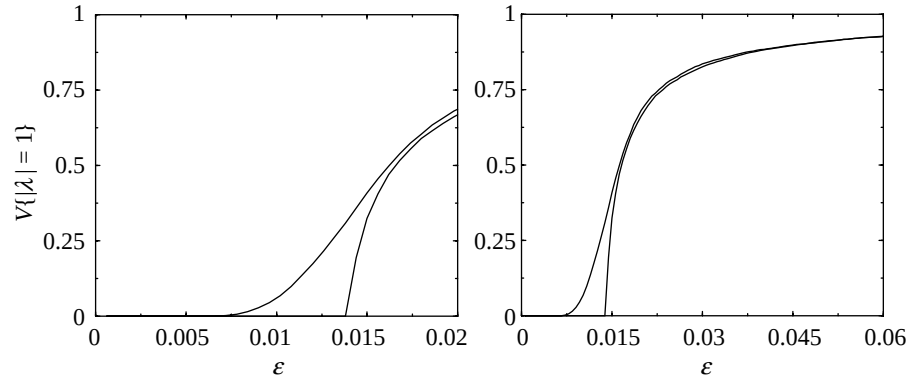

Figure 4. Volume fraction V of grains transformed into a single variant ($|\lambda| = 1$) as a function of ε. The upper and lower curves give fractions as they result from the full minimization process and the upper bound, respectively.

for $\mathcal{E}$, namely small ε and large ε, which are separated by an *intermediate regime*. More precisely, there is a constant c_{e} such that

$$\mathcal{E}(\varepsilon) \approx \mu c_{\mathrm{e}} \varepsilon^2; \tag{5.3}$$

for ε small, and the second derivative, $\mathcal{E}''(\varepsilon)$ approaches the limiting value 4μ as ε increases. We have obtained the value $c_{\mathrm{e}} = 0.38$ from our numerics.

It is easy to understand the mechanisms leading to the domains of quadratic dependence. For small values of ε none of the grains transforms to a single variant but to a mixture, that is, for such applied strains we have $|\lambda| < 1$ throughout (see (2.3)). This is clearly demonstrated by the upper curves in figure 4, which show the volume fraction

$$V = \frac{\#\{G : |\lambda(G)| = 1\}}{\#\{G \subseteq \mathcal{P}\}} \tag{5.4}$$

occupied by the grains transformed to a single variant as a function of the applied strain. Within this regime both the strains and transformation strains depend linearly on ε since, as can be checked easily, *the elasticity problem is linear in ε as long as $|\lambda| < 1$ throughout the polycrystal*. Linearity of the strains translates into quadratic behaviour for the energy, as indicated in (5.3).

For larger values of ε, a non-negligible fraction of the grains have transformed to a single variant and thus carry a transformation strain with $|\lambda| = 1$. Such grains cannot further deform through phase change, and they therefore give rise to an intermediate nonlinear regime in which some grains continue to undergo phase transitions while others do not. As ε continues increasing, further transformation becomes less and less likely (see figure 4). The curvature of the homogenized energy curve thus approaches that of a linearly elastic material and $\mathcal{E}''(\varepsilon)$ approaches the limiting value 4μ.

(It is of interest in this context to consider figure 5, which gives the crystallographic orientation and the transformation strains of a 10×10-grain window within our 1000×1000-grain polycrystal. Here we have assumed $\varepsilon = 0.005$; we see that most of the transformation occurs on favourably oriented crystallites.)

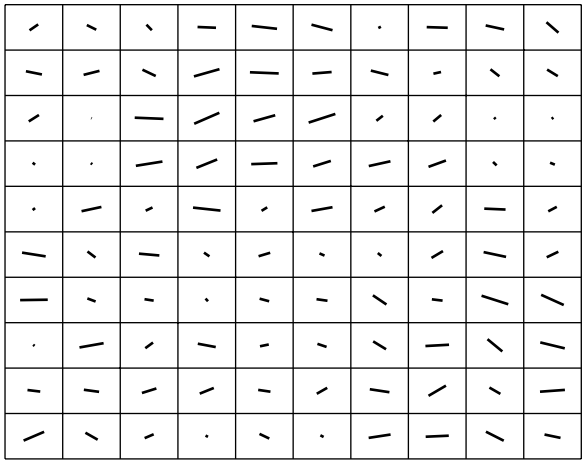

Figure 5. Microstructure in a 10×10 portion of a 1000×1000 polycrystal transformed under $\varepsilon = 0.005$. Lines indicate grain orientations, with lengths proportional to the absolute value of the corresponding twin-fraction λ.

(*b*) *Lower bound*

In § 4 *a* we have derived lower bounds L_1 and L_2 which are useful for small and large values of ε, respectively. These bounds are given by

$$L_1 = \frac{2\mu}{1-2\nu}(h^0)^2 + \mu(c_1(d_1^0)^2 + c_2(d_2^0)^2), \tag{5.5}$$

where the coefficients c_1 and c_2 are displayed in table 1, and

$$L_2 = \begin{cases} \dfrac{2\mu}{1-2\nu}(h^0)^2, & \text{if } 0 \leqslant d^0 \leqslant a\dfrac{2}{\pi}, \\ \dfrac{2\mu}{1-2\nu}(h^0)^2 + 2\mu\left(d^0 - a\dfrac{2}{\pi}\right)^2 & \text{if } d^0 \leqslant a\dfrac{2}{\pi}. \end{cases} \tag{5.6}$$

Our overall lower bound is therefore given by

$$L(\varepsilon^0) = \max\{L_1(\varepsilon^0), L_2(\varepsilon^0)\}. \tag{5.7}$$

As mentioned in § 4 *a* the constants c_1 and c_2 in (5.5) depend on the number $N_\mathrm{g} = n_\mathrm{g}^2$ of grains within each group in our decomposition of the polycrystal. In table 1 we display calculated values of these constants for different values of n_g. Details on the (rather interesting) computations needed in the evaluation of these constants are given in Appendix B.

(*c*) *The upper bound*

Like the homogenized energy, the upper bound obtained in § 4 *b* exhibits two main ranges of quadratic behaviour for $\mathcal{E}$, small ε and large ε, separated by an intermediate nonlinear regime. As shown in Appendix C, the upper bound is given by the quadratic form

$$U = \mu c_\mathrm{u}((d_1^0)^2 + (d_2^0)^2) \quad \text{for } d^0 \leqslant d^*, \tag{5.8}$$

Table 1. *Coefficients of the lower bound L_1 of equation (5.5) for various values of n_g*

n_g	c_1	c_2
3	0.084	0.057
4	0.14	0.12
5	0.17	0.15
6	0.20	0.18
7	0.22	0.20
8	0.23	0.22
9	0.25	0.24
10	0.26	0.25
11	0.27	0.26
12	0.28	0.27
13	0.29	0.28

where $c_u = 0.4974$ and $d^* = a \cdot 0.6263$. For large values of d_0, on the other hand, the curvature of the upper bound approaches that of the linear elasticity regime for reasons identical to those discussed in § 5 *a* in connection with the homogenized energy.

A deeper connection between $\mathcal{E}$ and its upper bound U emerges as we consider values of d^0 of the same order or larger than a. For such large values of d^0, the grains transform to one of the variants and not to a mixture of them (i.e. $|\lambda| = 1$ in (2.3)), and the choice between $\lambda = 1$ and $\lambda = -1$ depends mostly on the orientation of the grain. This implies that, in this regime, transformation strains from different grains are very nearly independent from each other (since the crystallographic orientations are independent) or, in other words, that the correlations between transformation strains of different grains are small. As a result, the minimizing distribution of transformation strains for the energy is quite close to the set of trial fields used in the derivation of the upper bound, and thus upper bound and homogenized energy agree very closely.

(*d*) *Numerical method: minimization, convergence and complexity*

Our numerical evaluation of the homogenized energy is presently applied to polycrystals with microstructure as described in § 4. This test case provides a concrete benchmark where many of the characteristic features of our method are tested. Additional refinements, which would be required in the treatment of general structures, are left for future work. In particular, our present tests give a clear picture of the stochastic structure of the problem and its interdependence with the microstructural details. (Further, it is quite reasonable to expect that even a somewhat restricted generalization of these methods—to corresponding three-dimensional polycrystals with cubic grains and variable transformation strains within grains—will lead to significant advance in our knowledge of phase transitions in polycrystalline structures.)

We are thus considering polycrystals with square grains and transformation strains with constant fractions λ. In view of the latter assumption, it is sufficient to use one element per grain, so that grains can be identified with discretization elements.

Our numerical method for the evaluation of $\mathcal{E}$ is based on the series of approximations $\mathcal{E}^{h,r}$ we introduced in § 3 (see equation (3.16)). To summarize our results in

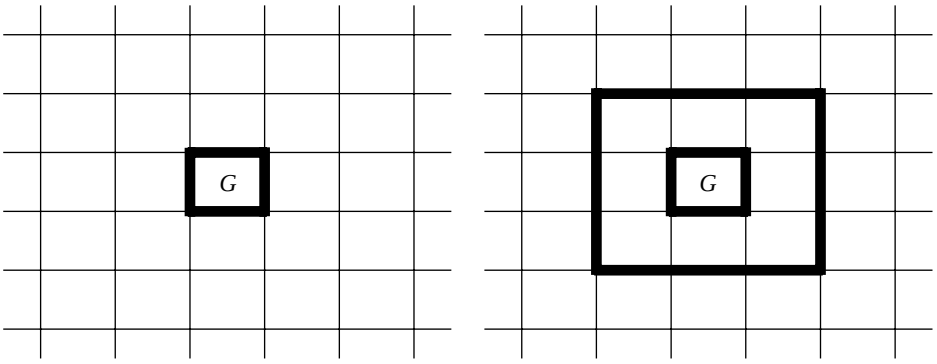

Figure 6. Local minimization groups corresponding to equation (5.10) with $r = 1$ and $r = 2$.

the context of the present test polycrystal we define the distance between two grains G_{ij} and $G_{k\ell}$ as (see (4.1))

$$\operatorname{dist}(G_{ij}, G_{k\ell}) = \max\{|i-k|, |j-\ell|\}.$$

Figure 6 shows all the grains whose distance to the grain G is less than r with $r = 1$ and $r = 2$. The (convergent) sequence of approximations $\mathcal{E}^{h,r}$ then arises as a result of the minimizations

$$\mathcal{E}^{h,r} = \min\{W^{h,r}([\lambda_{ij}]) : -1 \leqslant \lambda_{ij} \leqslant 1\}, \tag{5.9}$$

where

$$W^{h,r} = \frac{2\mu}{1-2\nu}(h^0)^2 + 2\mu[(d_1^0 - d_1^{\mathrm{T(av)}})^2 + (d_2^0 - d_2^{\mathrm{T(av)}})^2] + \mu \sum_{\operatorname{dist}(G,H)<r} a_{ij}^{GH}(d_i^{\mathrm{T}}(G) - d_i^{\mathrm{T(av)}})(d_j^{\mathrm{T}}(H) - d_j^{\mathrm{T(av)}}), \tag{5.10}$$

G and H are grains as in (4.1), and

$$d_1^{\mathrm{T}}(G_{ij}) = a\lambda_{ij}\cos(2\theta(G_{ij})) \quad \text{and} \quad d_2^{\mathrm{T}}(G_{ij}) = a\lambda_{ij}\sin(2\theta(G_{ij})). \tag{5.11}$$

The minimum indicated in (5.9) can be efficiently obtained through a rather simple minimization method, whose remarkable performance in our context can be understood, again, as resulting from the fast decay of correlations. Our minimization algorithm proceeds as follows: given a pair of integers (i, j), the strain energy $W^{h,r}$ is minimized with respect to the fraction λ_{ij} corresponding to the grain G_{ij} (with restrictions as indicated in (5.9)) while the rest of the variables $\lambda_{k\ell}$ are held fixed. This defines the new state of the fraction λ_{ij}, which is used in all subsequent calculations. Using a visiting schedule, the fractions λ of all the grains in the polycrystal are updated once per iteration. (Our computations use a lexicographic visiting schedule, but many other possibilities may be as efficient.) A (small) number of iterations of this process, finally, produces the minimum with the required accuracy.

For most optimization problems such a simple-minded algorithm would require an extremely large number of iterations. However, this is not the case here since, as a result of the fast decay of correlations in the minimizing distributions, our problem behaves effectively as a sum of well-conditioned quadratic problems in a

Table 2. *Convergence of the calculated energy values $\mathcal{E}^{h=1/n,r}$ as a function of the number I of minimization iterations*

I	$N=50^2$ $r=1$	$N=50^2$ $r=10$	$N=1000^2$ $r=1$	$N=1000^2$ $r=10$
1	1.676	1.523	1.682	1.524
2	1.240	1.020	1.242	1.005
3	1.229	0.990	1.230	0.965
4	1.229	0.986	1.230	0.959
5	1.229	0.984	1.230	0.957
6	1.229	0.984	1.230	0.957
7	1.229	0.984	1.230	0.957

small number of variables. Such fast convergence is demonstrated in the convergence studies of tables 2–4.

Our evaluation of the homogenized energy $\mathcal{E}$ results from a total of three approximating processes: (1) grain size $h = 1/n \to 0$; (2) number $r \to \infty$ of neighbours accounted for exactly in the approximation (5.10); and (3) number of iterations I in the minimization process. A few sets of numerical results, presented in what follows, will illustrate the convergence of the complete algorithm as these parameters are varied.

We consider first the convergence of the minimization algorithm as I is increased, for various values of n and r. Table 2 shows the computed energy value after iteration number $I = 1, 2, \ldots$, for a number $N = n^2$ of grains with $n = 50$ and $n = 1000$, and with $r = 1$ and $r = 10$. The behaviour shown in this table is representative of the most challenging cases we have encountered; the specific value of the applied strain is

$$\varepsilon^0 = \begin{bmatrix} 0.005 & 0 \\ 0 & -0.005 \end{bmatrix}. \tag{5.12}$$

These calculations, as well as all others in this paper, were initialized by the trivial distribution in which $\lambda_{ij} = 0$ throughout.

Table 2 shows that the number of iterations required by the minimization algorithm to obtain a given accuracy does not change with n, but may increase with r. To study the dependence of I on the parameter r, we display, in table 3, the number of iterations required to obtain an error smaller than 10^{-d} (for a fixed realization of $N = n^2$ grains) for various values of r when $n = 200$. We see that the dependence in r asymptotes to a constant as $r \to \infty$, so that I is effectively independent of r.

We now turn to a discussion of the convergence of $\mathcal{E}^{h,r}$ for fixed r as n tends to ∞. Table 4 shows the calculated values of $\mathcal{E}^{h,r}$ for different values of $n = 1/h$ and r, and for an applied strain as given in (5.12). Here we note that, since the orientations of the grains are random variables, the value of $\mathcal{E}^{h,r}$ obtained numerically will exhibit statistical fluctuations depending on the realization used in each particular example. This statistical dependence leads to a type of convergence typical of random systems. In addition to the convergence in the small-grain limit, table 4 also demonstrates the convergence as the truncating parameter r is increased. We see that a value of r as small as $r = 5$ leads to errors of the order of 1%.

As claimed in the introduction, the overall complexity of the method is of order $\mathcal{O}(N)$. Indeed, it can be shown easily that the first and second derivatives of $W^{h,r}$

Table 3. *Number I of iterations required to obtain an error smaller than 10^{-d} as function of the parameter r*

	$d=1$	2	3	4	5	6
$r=1$	1	2	3	3	4	5
2	1	2	3	4	5	5
5	2	3	5	7	8	11
10	2	4	6	8	12	15
20	2	4	6	8	12	15

Table 4. *Computed values of $\mathcal{E}^{h,r}$ for the applied strain (5.12) and for various values of N and r*

	$N=50^2$	100^2	200^2	500^2	1000^2
$r=1$	1.23	1.22	1.24	1.24	1.25
2	1.17	1.14	1.16	1.16	1.16
3	1.07	1.06	1.06	1.06	1.06
4	1.03	1.01	1.01	1.01	1.01
5	1.01	0.99	0.99	0.99	0.99
6	1.00	0.98	0.97	0.98	0.98
7	0.99	0.97	0.97	0.97	0.97
8	0.99	0.97	0.96	0.96	0.96
9	0.99	0.96	0.96	0.96	0.96
10	0.98	0.96	0.95	0.96	0.96
20	0.98	0.96	0.95	0.95	0.95
30		0.96	0.95	0.95	0.95

with respect to a single λ_{ij}, which are necessary for the explicit minimization respect to this one-dimensional variable, can be computed in $\mathcal{O}(r^2)$ operations. It immediately follows that the complexity of our method is $\mathcal{O}(r^2IN)$, where I is the number of iterations. As we have previously argued, I depends on the desired accuracy only and r can be chosen as a rather small integer, thus the linear complexity of the method on the number of grains. A direct demonstration of this linear complexity is given in table 5, which shows the overall computing times necessary to produce an error of less than 10^{-3} for a fixed realization of $N=n^2$ grains, and for different values of n and r. We see that a computation involving a number of as many as 1000 000 grains can be resolved with an error of less than 1% in *ca.* 30 min computation (on a 300 MHz PC). A 3 min computation, on the other hand, produces the energy values with an error of 5%.

We gratefully acknowledge support from NSF (through an NYI award and through contract nos DMS-9523292 and DMS-9816802). O.P.B. gratefully acknowledges support from the AFOSR (through contract nos F49620-96-1-0008 and F49620-99-1-0010) and from the Powell Foundation.

Appendix A. Strain-energy constants

Our evaluation of the coefficients a_{ij}^{EF} in equation (3.6) results, mainly, from the operations indicated in equation (3.3): differentiation of the Green's function with

Table 5. *Computing times for various values of N and r*

	$N = 10^2$	100^2	1000^2
$r = 1$	0.00	0.17	18.62
2	0.01	0.37	40.28
4	0.02	1.75	180.22
10		15.56	1940.37

respect to x_s, integration over F with respect to x', differentiation of the result with respect to x_u and, finally, integration with respect to x. Use of the deviatoric components (3.4) and algebraic rearrangement then leads to the explicit expressions mentioned in § 3 *a*, namely

$$a_{ij}^{EF} = a_{ij}(\boldsymbol{k}) = \sum_{0\leqslant i_1,i_2,i_3,i_4\leqslant 1} (-1)^{i_1+i_2+i_3+i_4} f_{ij}((k_1+i_1-i_2, k_2+i_3-i_4)h) + b_{ij}. \tag{A 1}$$

Here $\boldsymbol{k} = (k_1, k_2)$ denotes the product of $m = 1/h$ with the difference between the centres of the squares E and F, that is, for $E = \boldsymbol{e} + [0,h]^2$ and $F = \boldsymbol{f} + [0,h]^2$ we have $\boldsymbol{k} = m(\boldsymbol{e} - \boldsymbol{f})$. Further,

$$b_{11} = \frac{h^2}{(1-\nu)}, \quad b_{12} = b_{21} = b_{22} = 0,$$

and, denoting $r^2 = x^2 + y^2$,

$$f_{11}(x,y) = -\frac{r^2\log(r)}{2\pi(1-\nu)},$$
$$f_{12}(x,y) = \frac{x^2\tan^{-1}(y/x) - y^2\tan^{-1}(x/y)}{2\pi(1-\nu)},$$
$$f_{21} = f_{12} \quad \text{and} \quad f_{22} = -f_{11}.$$

Appendix B. Evaluation of the lower bound

Here we provide an explicit expression for the lower bound L_1 (see equation (4.22)). To do this we obtain, in Appendix B *a*, an explicit expression for the function F, and we derive, in Appendix B *b*, the Euler equations of the resulting variational problem. These equations allow us to reduce the evaluation of the lower bound to computation of averages of solutions of certain linear elasticity problems. A numerical method for the computation of these averages and corresponding explicit numerical values for the configurations considered in this paper, finally, are presented in Appendix B *c*.

(*a*) *The energy F for the traction-free configurations*

The function $F = F(\boldsymbol{\lambda}, \boldsymbol{\theta})$ was defined in equation (4.15). As explained in § 4 *a*, $F(\boldsymbol{\lambda}, \boldsymbol{\theta})$ equals the elastic energy contained in the union $A \in \mathcal{A}$ of a group of $N_\mathrm{g} = n_\mathrm{g}^2$ grains with crystallographic orientations given by the vector $\boldsymbol{\theta}$ and transformation strains determined by the vector $\boldsymbol{\lambda}$ (see equation (4.5), the paragraph preceding

equation (4.15) and figure 1). Explicitly, $F(\boldsymbol{\lambda}, \boldsymbol{\theta})$ equals F_A (see (4.12)), with ε^{T} as in (4.14) and associated displacement v as defined by (4.11).

To compute F we use the distributions $\gamma^{\mathrm{T}(i,j)} = \gamma^{\mathrm{T}(i,j)}(x)$ of transformation strains within A given by

$$\gamma^{\mathrm{T}(i,j)}(x) = \begin{cases} \gamma^{\mathrm{T}(i)}, & \text{if } x \in j\text{th square}, \\ 0, & \text{otherwise}, \end{cases}$$

where $i = 1, 2$ and

$$\gamma^{\mathrm{T}(1)} = \begin{bmatrix} 1 & 0 \\ 0 & -1 \end{bmatrix} \quad \text{and} \quad \gamma^{\mathrm{T}(2)} = \begin{bmatrix} 0 & 1 \\ 1 & 0 \end{bmatrix}.$$

Also, we denote by $v^{(i,j)}$ the solution of the traction-free problem in A with transformation strain $\gamma^{\mathrm{T}(i,j)}(x)$; that is, $v^{(i,j)}$ solves the equations

$$\left.\begin{aligned} \tau_{k\ell,\ell} &= 0, \\ \tau_{k\ell} &= c_{k\ell rs}(v^{(i,j)}_{r,s} - \gamma^{\mathrm{T}(i,j)}_{rs}), \\ \tau_{k\ell}(x)\hat{n}_\ell(x) &= 0, \quad x \in \partial A. \end{aligned}\right\} \tag{B 1}$$

We clearly have

$$v = a \sum_{j=1}^{N_{\mathrm{g}}} \sum_{i=1}^{2} \lambda_j \alpha_{ij} v^{(i,j)},$$

where

$$\alpha_{ij} = \begin{cases} \cos(2\theta_j), & \text{if } i = 1, \\ \sin(2\theta_j), & \text{if } i = 2. \end{cases}$$

Therefore,

$$F = \frac{1}{2|A|} \int_A c_{pqrs}(v_{p,q} - \varepsilon^{\mathrm{T}}_{pq})(v_{r,s} - \varepsilon^{\mathrm{T}}_{rs}) = a^2 D_{ijkl} \lambda_j \alpha_{ji} \lambda_\ell \alpha_{\ell k}, \tag{B 2}$$

where the summation is extended to $1 \leqslant i,\ k \leqslant 2$ and $1 \leqslant j,\ \ell \leqslant N_{\mathrm{g}}$, and the coefficients $D_{ijk\ell}$ are given by

$$D_{ijk\ell} = \frac{1}{2|A|} \int_A c_{pqrs}(v^{(i,j)}_{p,q} - \gamma^{\mathrm{T}(i,j)}_{pq})(v^{(k,\ell)}_{r,s} - \gamma^{\mathrm{T}(k,\ell)}_{rs}).$$

Equation (B 2) shows that F is a quadratic homogeneous function of $a\lambda_i \cos(2\theta_i)$ and $a\lambda_i \sin(2\theta_i)$, which can be evaluated directly once the constants $D_{ijk\ell}$ are known. We have computed these constants numerically by means of a straightforward finite-element method.

(*b*) *Euler equations and lower bound*

Having obtained an explicit expression for the function F in Appendix B *a* and since $\mathcal{L}$ is a convex functional, we may use variations to compute the minimum value

L_1 of $\mathcal{L}$ (see (4.22), (4.23)). It is thus easy to see that the minimizer $\boldsymbol{\lambda}^{(0)}$ satisfies the Euler equations

$$F_{\lambda_i} = \frac{4}{K} a\mu[(d_1^0 - d_1^{\mathrm{T(av)}})\cos(2\theta_i) + (d_2^0 - d_2^{\mathrm{T(av)}})\sin(2\theta_i)]. \tag{B 3}$$

We note that both the left- and right-hand sides of these equations depend on the unknown function $\boldsymbol{\lambda}^{(0)}$. More precisely, the left-hand sides depend on exactly one value of the function $\boldsymbol{\lambda}^{(0)}$, while the right-hand sides depend on certain averages involving the values of $\boldsymbol{\lambda}$ for all angles $\boldsymbol{\theta}$.

This infinite system of equations for the function $\boldsymbol{\lambda}$ can in fact be solved explicitly. To do this define the solutions $\boldsymbol{\lambda}^{(1)}$ and $\boldsymbol{\lambda}^{(2)}$ of the equations

$$F_{\lambda_i}(\boldsymbol{\lambda}^{(1)}) = \frac{4}{K} a^2\mu\cos(2\theta_i) \quad \text{and} \quad F_{\lambda_i}(\boldsymbol{\lambda}^{(2)}) = \frac{4}{K} a^2\mu\sin(2\theta_i). \tag{B 4}$$

Noting that (B 3) is a linear system of equations for $\boldsymbol{\lambda}$ (since F is a homogeneous quadratic function of this unknown), it follows that

$$\boldsymbol{\lambda}^{(0)} = \frac{(d_1^0 - d_1^{\mathrm{T(av)}})}{a}\boldsymbol{\lambda}^{(1)} + \frac{(d_2^0 - d_2^{\mathrm{T(av)}})}{a}\boldsymbol{\lambda}^{(2)}. \tag{B 5}$$

Taking appropriate averages of these equations—as indicated in (4.20)—we then obtain the relations

$$\left.\begin{aligned} d_1^{\mathrm{T(av)}} &= (d_1^0 - d_1^{\mathrm{T(av)}})I_1 + (d_2^0 - d_2^{\mathrm{T(av)}})I_2, \\ d_2^{\mathrm{T(av)}} &= (d_1^0 - d_1^{\mathrm{T(av)}})I_3 + (d_2^0 - d_2^{\mathrm{T(av)}})I_4 \end{aligned}\right\} \tag{B 6}$$

for the average deviators, where

$$\left.\begin{aligned} I_1 &= \left(\frac{2}{\pi}\right)^{N_\mathrm{g}} \frac{1}{N_\mathrm{g}} \sum_{j=1}^{N_\mathrm{g}} \int \lambda_j^{(1)}(\theta)\cos(2\theta_j)\,\mathrm{d}\theta, \\ I_2 &= \left(\frac{2}{\pi}\right)^{N_\mathrm{g}} \frac{1}{N_\mathrm{g}} \sum_{j=1}^{N_\mathrm{g}} \int \lambda_j^{(2)}(\theta)\cos(2\theta_j)\,\mathrm{d}\theta, \\ I_3 &= \left(\frac{2}{\pi}\right)^{N_\mathrm{g}} \frac{1}{N_\mathrm{g}} \sum_{j=1}^{N_\mathrm{g}} \int \lambda_j^{(1)}(\theta)\sin(2\theta_j)\,\mathrm{d}\theta, \\ I_4 &= \left(\frac{2}{\pi}\right)^{N_\mathrm{g}} \frac{1}{N_\mathrm{g}} \sum_{j=1}^{N_\mathrm{g}} \int \lambda_j^{(2)}(\theta)\sin(2\theta_j)\,\mathrm{d}\theta. \end{aligned}\right\} \tag{B 7}$$

These equations now permit us to obtain the average deviator and thus through (B 5) the minimizing function $\boldsymbol{\lambda}^{(0)}$ itself. Explicitly, we obtain

$$d_1^{\mathrm{T(av)}} = \frac{I_1}{1 + I_1} d_1^0 \quad \text{and} \quad d_2^{\mathrm{T(av)}} = \frac{I_4}{1 + I_4} d_1^0,$$

since, as we will show in Appendix B *c*, $I_2 = I_3 = 0$. The numerical method used for the (non-trivial) evaluation of the high-dimensional singular integrals I_1 and I_4 is described in Appendix B *c*.

Since F is a quadratic and homogeneous function of λ, we have

$$F = \tfrac{1}{2}\lambda_i f_{\lambda_i}. \tag{B 8}$$

In view of equations (B 3), (B 5) and (B 8), finally, the lower bound $L_1 = \mathcal{L}(\boldsymbol{\lambda}^{(0)})$ can be evaluated in terms of the integrals $I_1 \cdots I_4$ which, as mentioned above, are computed explicitly in Appendix B *c*. The corresponding values of the related constants

$$c_1 = 2/(1 + I_1) \quad \text{and} \quad c_2 = 2/(1 + I_4) \tag{B 9}$$

have been quoted in table 1; the resulting expression for the lower bound is

$$L_1 = \frac{2\mu}{1 - 2\nu}(h_1^0)^2 + \mu c_i (d_i^0)^2. \tag{B 10}$$

(*c*) *Evaluation of the angular integrals*

To obtain the integrals (B 7) required for the explicit evaluation of the lower bound (B 10) we first compute the quantities $\boldsymbol{\lambda}^{(1)}$ and $\boldsymbol{\lambda}^{(2)}$, which are solutions of the linear systems (B 4). Calling A the symmetric matrix associated with the quadratic form F, $F(\boldsymbol{\lambda}) = \boldsymbol{\lambda}^{\mathrm{T}} A \boldsymbol{\lambda}$, and calling $\boldsymbol{b}^{(1)}$ and $\boldsymbol{b}^{(2)}$ the vectors whose ith components are

$$b_i^{(1)} = \frac{2}{N_\mathrm{g}} a^2 \mu \cos(2\theta_i) \quad \text{and} \quad b_i^{(2)} = \frac{2}{N_\mathrm{g}} a^2 \mu \sin(2\theta_i), \tag{B 11}$$

these systems of equations can be expressed in the form

$$A\boldsymbol{\lambda}^{(i)} = \boldsymbol{b}^{(i)}. \tag{B 12}$$

Note that, like A and $\boldsymbol{b}^{(i)}$, the vectors $\boldsymbol{\lambda}^{(i)}$ depend on $\boldsymbol{\theta}$. As we will see, the linear system (B 12) does not admit solutions for certain values of $\boldsymbol{\theta}$; in what follows we thus study the dependence of the kernel of the matrix A on these angles.

Since A is positive semidefinite, $\boldsymbol{\lambda}$ belongs to the kernel of $A(\boldsymbol{\theta})$ if and only if $F(\lambda) = 0$. This means that the transformation strain associated with $\boldsymbol{\lambda}$ and $\boldsymbol{\theta}$ causes no stress or, what is the same, it produces a displacement of zero energy. This is only possible if the displacement in the ith square is equal to the corresponding transformation strain plus a translation and an infinitesimal rotation:

$$u = a\lambda_i \begin{bmatrix} \cos(2\theta_i) & \sin(2\theta_i) \\ \sin(2\theta_i) & -\cos(2\theta_i) \end{bmatrix} \begin{pmatrix} x_1 \\ x_2 \end{pmatrix} + \begin{bmatrix} 0 & -\beta_i \\ \beta_i & 0 \end{bmatrix} \begin{pmatrix} x_1 \\ x_2 \end{pmatrix} + \begin{pmatrix} c_1 \\ c_2 \end{pmatrix}.$$

Because of the necessary continuity of u across the boundaries of the squares, it can be checked that the kernel of $A(\theta)$ is different from zero if and only if there exist numbers $\lambda_{k\ell}$ with $0 \leqslant k, \ell \leqslant n_\mathrm{g} - 1$ and a constant C such that the following equations are satisfied:

$$\begin{aligned} \lambda_{k\ell} \sin(2\theta(G_{k\ell})) + \lambda_{(k+1)(\ell+1)} \sin(2\theta(G_{(k+1)(\ell+1)})) \\ = \lambda_{(k+1)\ell} \sin(2\theta(G_{(k+1)\ell})) + \lambda_{k(\ell+1)} \sin(2\theta(G_{k(\ell+1)})), \end{aligned} \tag{B 13}$$

$$\lambda_{k\ell} \cos(2\theta(G_{k\ell})) = C. \tag{B 14}$$

(For convenience here we have turned to a rectangular labelling of grains, in which the ith grain is $G_{k\ell}$ where $i = \ell n_\mathrm{g} + k + 1$. In an exception to the practice followed

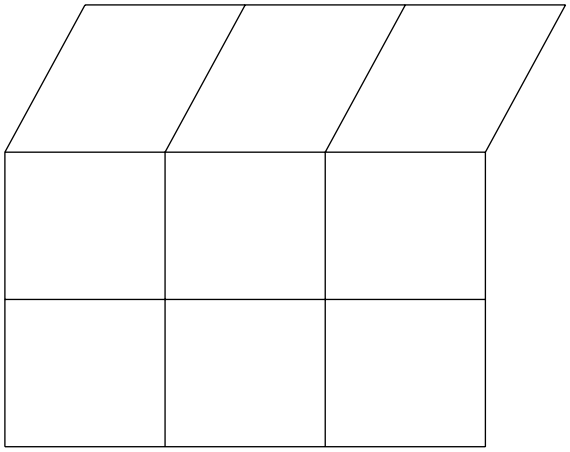

Figure 7. A zero-energy transformation pattern. The orientation of the upper row of grains equals $\theta = \frac{1}{4}\pi$, the remaining grains do not transform.

in the rest of the paper, the summation convention *is not* in force in the last two expressions.)

The first of the last two equations has to be satisfied for $0 \leqslant k,\ \ell \leqslant n_{\mathrm{g}} - 2$ and the last one for $0 \leqslant k,\ \ell \leqslant n_{\mathrm{g}} - 1$. The kernel of $A(\theta)$ thus consists of all the vectors $\boldsymbol{\lambda} = (\lambda_i)$ whose ith components equal $\lambda_{k\ell}$, where $i = \ell n_{\mathrm{g}} + k + 1$. In figure 7 we sketch a displacement of zero energy for $n_{\mathrm{g}} = 3$ and the orientations of the grains of the first row is $\frac{1}{4}\pi$. For future use we point out that, as can be seen from (B 11), if the constant C in equation (B 14) is equal to zero then the vector $b^{(2)}$ is not orthogonal to the kernel of A.

To study the convergence of the integrals I_i we define the set Θ by

$$\Theta = \{\theta : \ker(A(\boldsymbol{\theta})) \text{ is not } 0\}. \tag{B 15}$$

For every singular point $\boldsymbol{\theta}_0 \in \Theta$ and for every vector $\boldsymbol{b}$ for which the equation $A(\boldsymbol{\theta}_0)\boldsymbol{\lambda} = \boldsymbol{b}$ does not admit solutions, the quantity $\boldsymbol{\lambda}(\boldsymbol{\theta}_0 + y)$ tends to infinity as $y \to 0$. The fact that A is positive semidefinite, further, tells us that the first term in the asymptotic expansion of λ has the form

$$\lambda(\theta_0 + y) \sim \frac{\lambda_0}{\Phi(y)}, \tag{B 16}$$

where $\Phi(y)$ is a semidefinite quadratic function of y. It can be seen that the set $\{\Phi(y) = 0\}$ has the same codimension as the set Θ around any point θ_0 around which the set Θ is smooth. Further, the vector λ_0 in equation (B 16) belongs to the kernel of $A(\theta_0)$.

Given the previous remarks, it is not in principle clear whether the integrals in (B 7) are finite. As we will show in what follows, this is indeed the case whenever $n_{\mathrm{g}} \geqslant 3$. Our proof is given for the integral I_4; the other cases are treated analogously.

We first need to compute the codimension of Θ. To this end, we split Θ into two sets, Θ_1 and Θ_2, where Θ_1 is the set in which the constant C in equation (B 14) is 0 and Θ_2 is the rest of Θ. It is immediate that Λ_1 is exactly the set in which all the grains of one column or all the grains of one row have the orientation $\frac{1}{4}\pi$. This set has codimension n_{g}. On the other hand, the codimension of Θ_2 is bigger than n_{g}.

We next note that $b^{(2)}(\boldsymbol{\theta})$ is not orthogonal to the $\ker(A(\boldsymbol{\theta}))$ whenever $\theta \in \Theta_1$. Thus, since the integrand of I_4 is, up to a multiplicative constant, $\boldsymbol{\lambda}^{(2)}\boldsymbol{b}^{(2)}$, and given the behaviour of $\boldsymbol{\lambda}^{(2)}$ (see equation (B 16)), we conclude that for I_4 to be finite we need $n_{\mathrm{g}} \geqslant 3$. Even though Θ is not smooth everywhere, a more detailed analysis shows that the above condition ($n_{\mathrm{g}} \geqslant 3$) is sufficient.

We shall presently establish that the constants I_2 and I_3 vanish; the constants I_1 and I_4 will then be evaluated via a Monte Carlo integration method. Let us show that $I_2 = I_3 = 0$ in the case $n_{\mathrm{g}} = 3$; the general case follows immediately. To do this, we call P the permutation

$$P(x_1, \ldots, x_9) = (x_1, x_4, x_7, x_2, x_5, x_8, x_3, x_6, x_9) \tag{B 17}$$

(which corresponds to reflection across the diagonal), and we let H be the function

$$H(\theta_1, \ldots, \theta_9) = (\tfrac{1}{2}\pi, \ldots, \tfrac{1}{2}\pi) - P(\theta_1, \ldots, \theta_9). \tag{B 18}$$

By symmetry we then have

$$P(\lambda)A(H(\theta))P(\lambda) = \lambda A(\theta)\lambda \tag{B 19}$$

for all θ, and thus

$$A(H(\theta))P(\lambda^{(i)}) = P(b^{(i)}) = b^{(i)}(P(\theta)) = (-1)^i b^{(i)}(H(\theta)). \tag{B 20}$$

From this equation we conclude that

$$P(\lambda^{(i)}(\theta)) = (-1)^i \lambda^{(i)}(H(\theta)), \tag{B 21}$$

and then

$$\lambda^{(i)} b^{(j)} = P(\lambda^{(i)})P(b^{(j)}) = (-1)^{i+j}\lambda^{(i)}(H(\theta))b^{(j)}(H(\theta)) \tag{B 22}$$

and $I_2 = I_3 = 0$, as desired.

As mentioned above, the remaining (high-dimensional) integrals I_1 and I_4 were evaluated by means of a Monte Carlo method. Given the singular structure mentioned at the beginning of this section, it is particularly important to understand the convergence properties of such a method in our present case. To that end we have evaluated these integrals by classical numerical integration methods in the lower-dimensional cases $n_{\mathrm{g}} = 3$ and $n_{\mathrm{g}} = 4$. In these cases a careful account was taken of the complete singular structure of the integrands, integrations were divided in various regular domains, taking advantage of certain known singular terms in the singularity expansions. In sum, two reliable numerical algorithms were used in the cases $n_{\mathrm{g}} = 3$ and $n_{\mathrm{g}} = 4$, both of which provided results in complete agreement. For larger values of n_{g} the deterministic integration methods become prohibitively expensive. The Monte Carlo methods, on the other hand, converge even faster in these cases—owing to the higher codimension k of the singular set.

The resulting integrals were used to compute the constants c_1 and c_2 required in the expression for the lower bound L_1. Explicit values of these constants are displayed in table 1 of § 5 *b*.

Appendix C.

In § 4 *b* we reduced the evaluation of our upper bound to solution of the minimization problem

$$U = \min_{|\lambda| \leqslant 1} \langle W \rangle(\lambda). \tag{C 1}$$

Here

$$\begin{aligned}\langle W \rangle = {} & \frac{2\mu}{1-2\nu}(h^0)^2 + 2\mu[(d_1^0 - d_1^{\mathrm{T(av)}})^2 + (d_2^0 - d_2^{\mathrm{T(av)}})^2] \\ & + \frac{\mu}{(1-\nu)}\left[1 - \frac{\log(4)}{\pi}\right]\left[\frac{2}{\pi}\int_0^{\pi/2} (d_1^{\mathrm{T}}(\theta))^2 \,\mathrm{d}\theta - (d_1^{\mathrm{T(av)}})^2\right] \\ & + \mu\frac{\log(4)}{\pi(1-\nu)}\left[\frac{2}{\pi}\int_0^{\pi/2} (d_2^{\mathrm{T}}(\theta))^2 \,\mathrm{d}\theta - (d_2^{\mathrm{T(av)}})^2\right],\end{aligned} \tag{C 2}$$

where

$$d_1^{\mathrm{T}}(\theta) = a\lambda(\theta)\cos(2\theta) \quad \text{and} \quad d_2^{\mathrm{T}}(\theta) = a\lambda(\theta)\sin(2\theta) \tag{C 3}$$

and

$$d_1^{\mathrm{T(av)}} = \frac{2}{\pi}\int_0^{\pi/2} a\lambda(\theta)\cos(2\theta)\,\mathrm{d}\theta \quad \text{and} \quad d_2^{\mathrm{T(av)}} = \frac{2}{\pi}\int_0^{\pi/2} a\lambda(\theta)\sin(2\theta)\,\mathrm{d}\theta. \tag{C 4}$$

(Note that λ is a scalar variable in the present context.)

Let $\lambda(\theta)$ be the minimizer of this convex variational problem. Taking variations of $\langle W \rangle$ with respect to λ we see that

$$\lambda(\theta) = k_1\frac{\cos(2\theta)}{g(\theta)} + k_2\frac{\sin(2\theta)}{g(\theta)} \tag{C 5}$$

whenever $|\lambda(\theta)| < 1$. Here the constants k_1 and k_2 are given by

$$\begin{aligned} k_1 &= \frac{2}{a}\left[1 - \frac{\log(4)}{\pi}\right]d_1^{\mathrm{T(av)}} + \frac{4(1-\nu)}{a}(d_1^0 - d_1^{\mathrm{T(av)}}), \\ k_2 &= \frac{2}{a}\frac{\log(4)}{\pi}d_2^{\mathrm{T(av)}} + \frac{4(1-\nu)}{a}(d_2^0 - d_2^{\mathrm{T(av)}}),\end{aligned} \tag{C 6}$$

and the function g is given by

$$g(\theta) = 1 + \left(1 - \frac{\log 16}{\pi}\right)\cos(4\theta).$$

To obtain the minimizer we need the (unknown) average values $d_1^{\mathrm{T(av)}}$ and $d_2^{\mathrm{T(av)}}$ of the deviatoric components of the transformation strain.

As an example we present the complete derivation of the upper bound in the case $d_2^0 = 0$—from which it follows that $d_2^{\mathrm{T(av)}} = 0$. Since the maximum value of the function $\cos(2\theta)/g(\theta)$ is attained at $\theta = 0$, $\lambda(\theta)$ is given by equation (C 5) for all θ if and only if k_1 is less than $g(0)$. For such values of k_1 the average deviator is then given by

$$d_1^{\mathrm{T(av)}} = \frac{2}{\pi}\int_0^{\pi/2} a\lambda(\theta)\cos(2\theta)\,\mathrm{d}\theta = \frac{ak_1}{2b_1(b_1+b_2)}, \tag{C 7}$$

where we have defined

$$b_1 = \left(1 - \frac{\log(4)}{\pi}\right)^{1/2} \quad \text{and} \quad b_2 = \left(\frac{\log(4)}{\pi}\right)^{1/2}.$$

This equation, together with equation (C 6), allows us to find $d_1^{\mathrm{T(av)}}$ as a function of d_1^0, and the explicit expression for the upper bound as a function of the applied strain follows immediately:

$$U = \frac{2\mu}{1-2\nu}(h^0)^2 + \frac{2b_1b_2\mu}{[2(1-\nu)+b_1b_2]}(d_1^0)^2 = \frac{2\mu}{1-2\nu}(h^0)^2 + 0.4974\mu(d_1^0)^2. \quad \text{(C 8)}$$

To determine the range of values of d_1^0 for which this equation is valid, we note from equations (C 6), (C 7) that

$$d_1^0 = \frac{[2(1-\nu)+b_1b_2]}{b_1(b_1+b_2)}\frac{a}{4(1-\nu)}k_1. \quad \text{(C 9)}$$

As we pointed out above, equation (C 8) is valid if and only if the condition $k_1 \leqslant g(0)$ is satisfied. This condition, further, is equivalent to the relation

$$d_1^0 \leqslant d_1^* = 2\frac{[2(1-\nu)+b_1b_2]}{(b_1+b_2)}\frac{ab_1}{4(1-\nu)}, \quad \text{(C 10)}$$

which gives us the explicit domain of validity of equation (C 8).

For $d_1^0 > d_1^*$, on the other hand, λ is given by different analytic expressions in various angular intervals—which are determined by a certain angle θ_0 which depends on the applied strain d_1^0, and which will be determined below. Thus, λ is given by formula (C 5) for $\theta_0 < \theta < \frac{1}{2}\pi - \theta_0$:

$$\lambda = \begin{cases} 1, & \text{for } \theta < \theta_0, \\ -1, & \text{for } \theta > \frac{1}{2}\pi - \theta_0. \end{cases}$$

To find θ_0 we first compute $d_1^{\mathrm{T(av)}}$ as a function of d_1^0 and θ_0:

$$\begin{aligned} d_1^{\mathrm{T(av)}} &= \frac{2}{\pi}\int_0^{\pi/2} a\lambda\cos(2\theta)\,\mathrm{d}\theta \\ &= \frac{4}{\pi}\int_0^{\theta_0} a\cos(2\theta)\,\mathrm{d}\theta + \frac{4}{\pi}\int_{\theta_0}^{\pi/4} a\lambda\cos(2\theta)\,\mathrm{d}\theta \\ &= \frac{2}{\pi}a\sin(2\theta_0) + \frac{ak_1}{2b_1(b_1+b_2)} \\ &\qquad \times \left\{1 + \frac{2}{\pi(b_1-b_2)}\left[b_2\tan^{-1}\left[\frac{b_2}{b_1}\tan(2\theta_0)\right] - 2b_1\theta_0\right]\right\}. \end{aligned} \quad \text{(C 11)}$$

We now use (C 6) and (C 11) to obtain k_1 as a function of d_1^0 and θ_0 and then we find θ_0 as a function of d_1^0 by solving the equation $\lambda(\theta_0) = 1$—where λ is given by formula (C 5). Having obtained $\lambda = \lambda(\theta)$, we may now evaluate the upper bound U presented in § 5.

To conclude we remark that the same ideas applied in the general case lead to the upper bound

$$U = \frac{2\mu}{1-2\nu}(h^0)^2 + \frac{2b_1b_2\mu}{[2(1-\nu)+b_1b_2]}[(d_1^0)^2 + (d_2^0)^2] \tag{C 12}$$

in the domain $(d_1^0)^2 + (d_2^0)^2 \leqslant (d^*)^2$, where

$$d_1^* = 2\frac{[2(1-\nu)+b_1b_2]}{(b_1+b_2)}\frac{ab_2}{4(1-\nu)}. \tag{C 13}$$

We note that, although this expression for the upper bound exhibits an isotropic dependence on the (small) applied strains, the bound is slightly anisotropic for larger applied strains for which this equation does not hold.

References

Arlt, G. 1990 Twinning in ferroelectric and ferroelastic ceramics: stress relief. *J. Mater. Sci.* **25**, 2655–2666.

Bhattacharya, K. & Kohn, R. V. 1997 Elastic energy minimization and the recoverable strains of polycrystalline shape-memory materials. *Arch. Ration. Mech. Analysis* **139**, 99–180.

Bowles, J. S. & Mackenzie, J. K. 1954 The crystallography of martensite transformations. I. *Acta Metall.* **2**, 129–137.

Bruno, O. P., Reitich, F. & Leo, P. 1996 The overall elastic energy of polycrystalline martensitic solids. *J. Mech. Phys. Solids* **44**, 1051–1101.

Eshelby, J. D. 1957 The determination of the elastic field of an ellipsoidal inclusion, and related problems. *Proc. R. Soc. Lond.* A **241**, 376–396.

Khachaturyan, A. G. 1967 Some questions concerning the theory of phase transformations in solids. *Sov. Phys. Solid State* **8**, 2163–2168.

Leo, P. H., Shield, T. W. & Bruno, O. P. 1995 Transient heat transfer effects on the pseudoelastic behavior of shape-memory wires. *Acta Metall. Mater.* **41**, 2477–2485.

Roitburd, A. L. 1973 Domain structure caused by internal stresses in heterophase solids. *Physica Status Solidi* A **16**, 329–338.

Smyshlyaev, V. P. & Willis, J. R. 1998 A 'non-local' variational approach to the elastic energy minimization of martensitic polycrystals. *Proc. R. Soc. Lond.* A **454**, 1573–1613.

Wayman, C. M. 1964 *Introduction to the crystallography of martensitic transformations.* London: Macmillan.

Wechsler, M. S., Lieberman, D. S. & Read, T. A. 1953 On the theory of the formation of martensite. *Trans. AIME* **197**, 1503–1529.